Published in final edited form as:
Curr Metabolomics. 2014 April ; 2(1): 53–69. doi:10.2174/2213235X02666140301002510.

Recent Advances in Metabolic Profiling And Imaging of Prostate Cancer

Roopa Thapar[1] and **Mark A Titus**[2]

[1]Department of Biochemistry and Cell Biology, Rice University, Houston, TX 77251-1892, USA

[2]Department of Genitourinary Medical Oncology, The University of Texas M.D. Anderson Cancer Center, Houston TX 77030, USA

Abstract

Cancer is a metabolic disease. Cancer cells, being highly proliferative, show significant alterations in metabolic pathways such as glycolysis, respiration, the tricarboxylic acid (TCA) cycle, oxidative phosphorylation, lipid metabolism, and amino acid metabolism. Metabolites like peptides, nucleotides, products of glycolysis, the TCA cycle, fatty acids, and steroids can be an important read out of disease when characterized in biological samples such as tissues and body fluids like urine, serum, etc. The cancer metabolome has been studied since the 1960s by analytical techniques such as mass spectrometry (MS) and nuclear magnetic resonance (NMR) spectroscopy. Current research is focused on the identification and validation of biomarkers in the cancer metabolome that can stratify high-risk patients and distinguish between benign and advanced metastatic forms of the disease. In this review, we discuss the current state of prostate cancer metabolomics, the biomarkers that show promise in distinguishing indolent from aggressive forms of the disease, the strengths and limitations of the analytical techniques being employed, and future applications of metabolomics in diagnostic imaging and personalized medicine of prostate cancer.

Keywords

Biomarker; Castration-Resistant Prostate Cancer; Magnetic Resonance Spectroscopy; Mass Spectrometry; Metabolomics; Metabolic Imaging; Nuclear Magnetic Resonance; Prostate Cancer

Introduction

In the United States, prostate cancer (PCa) is the second leading cause of cancer-related deaths in men, the first being lung cancer. In the American Cancer Society's 2013 annual report, they estimated that 238,590 new cases of prostate cancer would be diagnosed and 29,720 men would die from the disease (http://www.cancer.org/cancer/prostatecancer/detailedguide/prostate-cancer-key-statistics). Increased screening of males over the age of

*Address correspondence to: Roopa Thapar, PhD, Tel: 713-201-7875; rthapar@rice.edu or Mark A Titus, PhD, Tel: 713-792-4467; mtitus1@mdanderson.org.

Conflict of Interest
The authors declare no competing financial interest.

50, and early detection of mostly indolent PCa has led to a large disparity between the estimated incidence of prostate cancer and lethality due to metastatic disease. A large proportion of men that are diagnosed with PCa have indolent disease that may never develop into an aggressive cancer phenotype. Many of these men will undergo invasive procedures for diagnosis and prophylactic treatment that may be unwarranted. Therefore, there is a need for new non-invasive methods that allow for better screening strategies as well as new biomarkers that can distinguish between indolent and aggressive metastatic forms of PCa. The ultimate goal of current research is to minimize false positives, to treat only those men who are at the greatest risk for aggressive forms of prostate cancer, and reduce testing and treatment for those at low risk for the disease.

Limited options are currently available for clinicians to screen for indolent vs. aggressive forms of PCa. Prostate cancer screening is commonly done by the prostate-specific antigen (PSA) blood test. The PSA test was developed in the 1980s (Fig. 1) when it was determined that a protein biomarker encoded by the prostate-specific gene kallikrein 3 (*KLK3*)[1] was secreted by the prostate gland into the serum only when the prostate gland underwent a change in tissue architecture due to either tumorigenesis, inflammation, or an enlarged prostate, as is observed in benign prostate hyperplasia (BPH)[2, 2b]. The PSA test along with a digital rectal exam (DRE), tissue biopsy and histopathology are commonly used for prostate cancer diagnosis[3]. Several variations of the PSA, such as determining the ratio of the free vs. α1-antichymotrypsin complexed PSA in the serum (fPSA and cPSA, respectively)[4,5,6], PSA velocity (PSAV), and PSA doubling time (PSADT) are also used[7]. The PSA test combined with the DRE has high sensitivity (i.e. is able to detect true positives), but has poor specificity (ability to detect true negatives) towards aggressive metastatic disease. It is not a useful approach in distinguishing indolent from aggressive disease. In addition, grading tissue morphology to give a Gleason score is the sole mechanism by which metastatic PCa is further classified. More robust prognostic markers are required to determine the degree of aggressiveness of the disease.

For these reasons, there has been much interest in the identification of new biomarkers that are non-invasive and can stratify patients with high sensitivity and specificity for screening, diagnosis, prognosis, prediction, and monitoring of aggressive and advanced prostate cancer (Fig. 1)[8]. Some of the promising new biomarkers that have been clinically evaluated include the long non-coding RNA prostate cancer antigen 3 (*PCA3*)[9,10], the *TMPRSS2-ERG* gene fusion[11], α-methyl-coenzyme A racemase (AMACR)[12, 12a], circulating tumor cells (CTCs) in the blood stream[13], and prostate derived exosomes[14] generated from the prostate and secreted into the blood. Of these, *PCA3* is most promising, is non-invasive as it is readily detected in urine of patients with metastatic disease (but not in BPH), and can be used in conjunction with the PSA test for prostate cancer screening[15,16,17].

Metabolite biomarkers have been successfully used in the clinic for prostate cancer diagnostic imaging. ^{18}F-fluoro-2-deoxyglucose (FDG) is commonly used in positron emission tomography (PET) and accumulates to high levels in tumors[18] due to the increased import of glucose into tumors by glucose transporters such as GLUT1. Hyperpolarized [1-^{13}C]-pyruvate may be a valuable metabolite as a diagnostic imaging tool, as has recently been shown in the first clinical study in men[19]. When the ratio of [1-^{13}C]-lactate/[1-^{13}C]-

pyruvate was measured after injection of hyperpolarized [1-^{13}C]-pyruvate, it was found to be significantly elevated in men with metastatic disease as opposed to men with low-grade tumors[19]. Several other metabolites are currently being screened for diagnostic imaging in preclinical models[20, 20a]. Metabolite levels of citrate[21,22,23,24,25,26,27], choline[28,29], glutamate[30], taurine[30], and sarcosine[31] in body fluids, such as urine and serum, as well as in tissue biopsies have been correlated with PCa progression and the change in levels of these metabolites, when analyzed globally, could be a potential strategy for distinguishing indolent from aggressive disease.

In this review, we will highlight recent studies using nuclear magnetic resonance (NMR) spectroscopy and mass spectrometry (MS) that hold promise for characterization of the prostate cancer metabolome and for imaging prostate cancer.

Cancer Metabolism: At the crossroads of genomics and proteomics

Why is cancer metabolism relevant? Several studies show that the metabolic properties of cancer cells i.e. aerobic glycolysis, lipid, and amino acid metabolism differ from normal cells and this may be valuable in cancer diagnosis and treatment. In 1931, the biochemist Otto Warburg was awarded the Nobel Prize in Physiology or Medicine "for his discovery of the nature and mode of action of the respiratory enzyme". Although he made seminal discoveries in respiration, cell physiology, and metabolism, he is known mostly for his careful observation that cancer cells consume more glucose and secrete more lactate compared to normal cells, even in the presence of excess oxygen that should in fact metabolize all of the glucose to CO_2[32,33] via mitochondrial oxidative phosphorylation. This observation is called the “Warburg effect”. Since Otto Warburg’s important discovery, it is now well established based on numerous reports that cancer cells show increased flux in metabolizing higher levels of glutamine driven at least in part due to higher energy demands and its involvement in anaplerotic reactions such as conversion to α-ketoglutarate, have increased lipid synthesis, and enhanced amino acid transport compared to normal cells[34,35,36]. The increased uptake of glucose in cancer is in large part due to the up-regulation of glucose transporters such as GLUT1[37,38,39]. The hypoxic conditions that exist in many tumors also increases the levels of the hypoxia inducible factors HIF1α and HIF2α, which in turn up-regulates enzymes of the glycolytic pathway, promoting glycolysis[40,41]. This reprogramming of cellular metabolism (Fig. 2) is now an emerging hallmark of cancer[42], and is intimately linked to changes in the proteome and the genome[43].

An important link between cancer metabolism and cancer genomics was established from sequencing efforts that identified missense mutations in the genes *IDH1* and *IDH2* in >70% of glioblastomas, oligodendrogliomas, and astrocytomas[44,45]. These genes encode for the metabolic enzymes isocitrate dehydrogenase, IDH1 and IDH2, respectively. The mutations encode for a single amino acid (R132 in IDH1 and R172 in IDH2) in the active site of IDH that alters its biochemical properties. The normal function of IDH1/2 is to oxidize isocitrate to α-ketoglutarate (α-KG) (Fig. 2, Fig. 3A). α-KG is a component of the tricarboxylic acid (TCA) cycle, is linked to glutamate via anaplerotic reactions, but it is also a substrate for more than 50 mammalian dioxygenases, such as TET2 that hydroxylates 5-methyl cytosine, the histone demethylases KDM, the prolyl hydroxylases EGLN 1/2/3, and the histone

methyltransferases KMT[46,47]. These enzymes directly regulate gene expression by controlling methylation of histones and DNA. The EGLN family also regulates HIF family proteins that are involved in several cancers. Intriguingly, mutant forms of IDH convert isocitrate to the R-enantiomer of 2-hydroxyglutarate (2HG), the first known oncometabolite[48]. 2HG competitively inhibits the normal functions of α-KG and is found in high levels in several cancers (Fig. 3A). Recently, genome-wide CpG methylation sequencing of chondrosarcoma biopsies has shown that IDH2 mutations are linked to DNA hypermethylation at CpG islands which are associated with genes implicated in stem cell maintenance, differentiation, and lineage specification[49].

Loss-of-function mutations have also been identified in all four subunits of the succinate dehydrogenase (*SDH*) complex in paragangliomas[50,51]. The SDH complex converts succinate to fumarate in the TCA cycle. Mutations in the fumarate hydratase (*FH*) gene are also linked to renal cell carcinomas, uterine, and skin cancer[52]. The exact mechanisms by which these mutant enzymes affect biochemical pathways are unclear, although SDH and FH have been suggested to act as tumor suppressors. High levels of succinate and fumarate accumulate in cancers that harbor mutant forms of SDH and FH and these cancers also show increased activity of HIF proteins and altered AMPK-signaling[53]. Two metabolic enzymes that are highly expressed in prostate cancer are phosphofructo-2-kinase/ fructose-2,6-bisphosphatase 3 (PFKFB3) and fatty acid synthase (FAS)[54]. PFKFB3 maintains the flux of fructose-2,6-bisphosphate in glycolysis whereas FAS promotes fatty acid synthesis.

In addition to metabolic enzymes, the metabolites themselves are associated with tumorigenesis. Pyruvate is the end product of glycolysis and links glycolysis to the TCA cycle. The pyruvate dehydrogenase complex (PDH) oxidizes and decarboxylates pyruvate to acetyl-CoA, which enters the TCA cycle (Fig. 3B). The pyruvate “hub” is a pivotal point that affects a number of metabolic pathways. Recent studies have shown that high rates of pyruvate oxidation augment oncogene-induced senescence (OIS), which prevents tumor progression[55]. Surprisingly, in the study by Kaplon et al[55], pyruvate oxidation was directly involved in inducing OIS. Two enzymes control the pyruvate flux: the kinase, PDK1 that phosphorylates PDH, thereby inactivating it, and the phosphatase, PDP2 that activates PDH (Fig. 3B). Knockdown of PDK1 results in increased flux of pyruvate into the TCA cycle and prevents tumor formation in $BRAF^{v600E}$ melanoma cell lines. Conversely, increasing the expression of PDK1 promotes tumorigenesis. Therefore, pyruvate levels can either inhibit or induce tumorigenesis, providing the first direct evidence for the active involvement of a metabolite in tumor progression. Acetyl-CoA, the product of pyruvate oxidation in the mitochondria is also produced by acetyl-CoA synthetases and ATP-citrate lyase in the nucleus. It is essential for lipid synthesis as well as acetylation of proteins, such as histones that control gene expression[56,57]. Finally, metabolic pathways can directly affect cell signaling by controlling ATP levels and the ATP/ADP ratio. ATP is required for posttranslational modifications. Phosphorylation, ubiquitination and other modifications are ATP-dependent reactions, which regulate important signaling networks that contribute to oncogenesis.

These studies have begun to unravel how cancer metabolism is closely interlinked with changes in the genome and proteome and how it may play a crucial role in tumor

progression. It also offers new opportunities for cancer drug discovery, diagnosis, and prognosis.

Metabolism in Prostate Cancer Cells

The human prostate gland is a walnut sized exocrine gland of the male reproductive system. The prostate anatomy has been described in terms of four zones[58]: the outermost zone consists of nonglandular anterior fibromuscular stroma and is responsible for 0% of PCa, the peripheral zone makes up ~70% of the gland and is responsible for 70–80% of PCa, the central zone makes up about 25% of the prostate and is responsible for only 2–3% of PCa, and the transition zone is ~5% of the gland and is mainly responsible for benign prostate hypertrophy (BPH). Approximately 10–20% of prostate cancers also originate from this zone. Prostatic fluid is produced by the secretory epithelium of the peripheral zone. It is slightly acidic (pH ~6.5)[59] and comprised mostly of sugars like fructose, with less than 1% protein content[59]. Biomarkers such as the glycoproteins prostatic acid phosphatase (PAP) and PSA are components of the prostatic fluid[60]. A unique feature of prostatic fluid from normal and BPH prostates is that it contains very high levels of citrate (Cit) (8000–15000 nmol/g of tissue)[61] as compared to other tissues where the citrate content is only 150–450 nmol/g. This is due to inhibition of mitochondrial (m-) aconitase, which converts citrate to isocitrate in the TCA cycle[62]. High levels of zinc in prostatic fluid (500–1000 times that in blood) inhibit the m-aconitase activity[63,64]. In contrast to normal cells, malignant prostate cells oxidize citrate in the TCA cycle, and citrate levels decrease to 1000–2000 nmol/g[65]. The levels of zinc are also low, in large part due to decreased expression of zinc transporters in the malignant prostate[66]. In addition, due to increased demand for lipid synthesis in malignant cells, spermine (Spm)[67,27] and phosphocholine (PCho) and total choline containing compounds (tCho) levels are significantly higher in PCa as compared to normal prostate[68,69,28,29,70]. Intriguingly, PCho and tCho levels are correlated with the tumor microenvironment. Hypoxia and acidic pH has been shown to regulate choline metabolism in a human prostate cancer xenograft model by regulating choline kinase-α expression by HIF1[71]. Prostate cancer cells also show increased uptake of choline, in part due to increased expression of choline transporters[69a]. Choline metabolic pathways are shown in Fig. 4. Other metabolites that have been reported to be markers for PCa vs. normal and BPH prostate tissues include sarcosine[31], lactate[21], taurine[30], glutamate[30], lysine[29], myo-inositol[27], and omega-6-fatty acids[72], all of which may be present at significantly higher levels in PCa tissues.

A unique feature of prostate, breast, and thyroid cancers is that at least in the initial stages, they are hormone-dependent. Charles Huggins and colleagues showed in the 1930s and 1940s[73,74] that the growth and metabolism of prostatic cells respond to testosterone and other androgens. A prostatic cell that is normal or castrate has a low metabolic rate and does not secrete. However, in the presence of testosterone or dihydrotestosterone, the cell grows larger and its metabolic rate increases. The effects of hormone on cell size, growth, and metabolism were found to be reversible. The discovery of 5-α-reductase enzymes[75,76,77] and the “active” androgen dihydrotestosterone (DHT)[78,79] were important milestones in understanding how the prostate gland may be regulated by androgens. Cloning of the androgen receptor (AR)[80,81,82], a hormone activated transcription factor and a key regulator

of androgen-dependent growth proved Huggins' original observations, revolutionized our understanding of PCa, and led to the development of novel cancer therapeutics. AR is implicated in both endocrine and paracrine stages of PCa malignancy. In a recent model proposed by C. Logothetis et al[83], the progression of prostate cancer from an endocrine driven androgen-dependent early stage cancer to one that is paracrine-driven and microenvironment dependent is a pivotal point at which the disease has manifested a more lethal phenotype. The paracrine-driven phase eventually leads to an autonomous phase that is no longer androgen dependent and is characterized by cell cycle changes in an advanced metastatic form of the disease. Careful analysis of metabolic profiles including the levels of androgens in each of these phases may provide new insights into disease progression and may be beneficial for surveillance. A characteristic feature of prostate cancer is that it has a propensity to metastasize to bone where it promotes osteoblast proliferation. A global GC–MS-based metabolic profiling study has identified elevated levels of cholesterol (a precursor of androgen biosynthesis) to be a signature of PCa that has metastasized to bone[84]. Although these studies have provided preliminary insights into metabolic changes that may occur in PCa, much remains to be done to correlate how metabolic changes in energy metabolism and steroids are linked to tumor aggressiveness and disease progression.

Methods in Metabolic Profiling and Imaging

(I) NMR and MS based metabolomics studies of PCa

Nuclear Magnetic Resonance (NMR) Spectroscopy and Mass Spectrometry (MS) are the two commonly used analytical techniques for metabolic profiling[85,86,87]. The two techniques are complementary and when used together offer the best approach to sample polar and non-polar metabolites over a wide concentration range. The main advantage of MS is that it has very high sensitivity, requires very little sample, and can detect low abundance metabolites in the 10^{-12} – 10^{-15} M range. A chromatographic step is usually performed before MS, and gas chromatography-MS (GC-MS), liquid chromatography-MS (LC-MS; ultrahigh-performance LC, UPLC-MS or high-performance LC, HPLC-MS) or capillary electrophoresis-MS (CE-MS) are the commonly used separation-coupled techniques. MS can be efficiently used for quantification of lipids and steroids, which are more difficult to quantify by NMR, although labeled standards are required. A major disadvantage of MS is that it requires extensive processing of the samples. All platforms require deproteinization and MS platforms such as GC-MS require derivitization. In contrast to MS, NMR has low sensitivity and requires that the metabolites be present in the μM concentration range for detection. The NMR spectrum of body fluids or tissue extracts consists of a complex mixture of different metabolites, each of which can be identified as a distinct pattern of resonances or peaks present at different frequencies with unique chemical shifts or p.p.m values (Fig. 5). NMR active nuclei that occur at natural abundance, and are commonly monitored, are ^{1}H and ^{31}P, and to a lesser extent ^{13}C. The area under the peak is related to the abundance of the metabolite and can be quantified. However, the NMR spectrum is usually very complex as it has information about all the metabolites in a single spectrum. In spite of these limitations, NMR is highly quantitative, requires little sample preparation and no derivatization in comparison to MS, and is highly reproducible. NMR is also amenable to high throughput analysis. Techniques such as high-resolution magic angle

spinning (HR-MAS) NMR can be performed on intact tissues[88], thereby circumventing the need for metabolite extraction procedures that can result in significant errors due to sample losses. MAS is a specialized technique that involves placing the samples at the magic angle of 54.74° with respect to the external magnetic field and spinning it at rates of 1–70 kHz/s. This leads to narrower signals, increasing spectral resolution. In addition, since NMR is a non-destructive technique, the intact tissue can be further utilized for either MS or immunohistochemistry analysis. Hyperpolarized NMR techniques have been employed to quantify metabolites[89,90,91,92] *in vitro* and *in vivo* as well as for diagnostic applications in cancer imaging[19,93]. Both NMR and MS have been used in metabolite targeted (i.e focused on select chemical classes) and untargeted approaches to study metabolites present in prostate tissue biopsies, blood plasma, and urine. A target list of metabolites is identified based on known standards and the data from NMR and MS is subjected to multivariate statistical analyses such as principal component analysis (PCA) to identify associations with outcomes such as disease state that may be statistically significant. The main goal of NMR and MS studies is to identify metabolite biomarkers that can risk-stratify patients as having benign, localized PCa, or metastatic PCa.

(Ia) Characterization of the Prostate Cancer Metabolome by MS—One of the most extensive chemometric studies to date was performed by Sreekumar et al[31] using high-throughput LC-MS and GC-MS. In this study, the authors profiled 1126 metabolite features from 262 clinical samples, consisting of 42 tissue biopsies and 110 matched samples of post-DRE urine and plasma from biopsy-positive and biopsy-negative individuals. The data from plasma and urine samples had a very high false discovery rate (99% for plasma and 67% for urine) and no significant differences were observed in these cohorts. Analysis of the 42 tissue biopsies indicated that 87 out of the 518 measured metabolites showed significant differences between PCa and benign tissues. A comparison of metastatic PCa and localized PCa tissues indicated that 124 of the 518 metabolites showed increased levels in metastatic PCa, whereas the levels of 102 of the 518 metabolites were significantly decreased. Although several hundred metabolites remain to be identified, a panel of six metabolites namely sarcosine, uracil, kynurenine, glycerol-3-phosphate, leucine, and proline showed a statistically significant increase in abundance in localized and metastatic PCa, as compared to benign tissues. The metabolic abundance profiles suggested that alteration of amino acid metabolism and methyl transferase activity is a hallmark of prostate cancer progression. In particular, sarcosine, an N-methyl derivative of glycine, appeared to be a candidate biomarker that showed promise in distinguishing between benign and metastatic PCa. The authors followed through with a targeted MS approach that quantified sarcosine levels in 89 tissue samples (36 PCa, 25 benign, and 28 metastatic). Whereas sarcosine was not detected in benign tissue, a significant increase in sarcosine levels in PCa and metastatic tissue samples was reported, corroborating their untargeted approach. Furthermore, sarcosine levels in the urine also followed the same trend as that observed in tissue biopsies. This study suggested that sarcosine could be a potential prognostic biomarker that could be detected non-invasively in the urine and may be a useful approach to follow PCa disease progression.

Since the original study by Sreekumar and colleagues was published, Jentzmik et al[94,95] reported contradictory findings in which no correlation was observed between sarcosine levels in either post-DRE urine or tissues, with prostate cancer aggressiveness. Cao et al[96] also reported a modest correlation between sarcosine levels and PCa progression, and the prognostic value of sarcosine was found to be inferior to the more robust PCA3 and fPSA biomarkers. In a study published this year, McDunn et al[97] examined over 500 tissue biopsies using UHPLC-MS/MS and GC-MS metabolomic platforms. The metabolomic profiles were correlated with PCa aggressiveness using Gleason scores as well as pathology data. Similar to the Sreekumar et al report[31], 52 metabolites identified were common in the two studies, and these showed a significant change in abundance in metastatic vs. benign tissues. PCa metastasis was also correlated with changes in amino acid and lipid metabolism in the McDunn study. In particular, elevated levels of glycerol-3-phosphate, sarcosine, kynurenine, proline, threonine, and uracil were found to be a characteristic feature of metastatic PCa in both[31,97] untargeted metabolomics studies. However, sarcosine levels were elevated only in tissue biopsies with a Gleason pattern of 8 or worse in the McDunn et al report. Therefore, the value of sarcosine as a prognostic marker for PCa progression is controversial.

The advanced stages of prostate cancer are distinguished by metastasis to bone. The first study to characterize metabolic changes that occur in bone due to PCa metastasis was performed by Thysell et al[84] using a GC-MS platform. In this study, 123 metabolites were profiled from 14 patients who had either hormone-naïve or castration-resistant PCa. Similar to the other studies, the metabolic changes in bone were related to alterations in amino acid and lipid metabolism. In particular, high levels of cholesterol, myo-inositol-1-phosphate, citric acid, fumarate, glycerol-3-phosphate, and fatty acids were found in PCa bone metastases samples compared to normal bone. High levels of several amino acids, such as glutamic acid, phenylalanine, and taurine were also found in PCa bone metastasis tissue. Of these metabolites, changes in cholesterol levels were most remarkable. Since increased cholesterol levels have previously been associated with PCa[98], and cholesterol uptake[99] and its biosynthesis are regulated by androgen levels and the androgen receptor[100,101], the results from the metabolic study are noteworthy. The Thysell et al study highlighted the role of cholesterol metabolism in advanced PCa, however neither cholesterol nor sarcosine were determined to be prognostic markers for metastatic PCa.

These studies illustrate how MS based approaches can be used to characterize the PCa metabolome. However, variability in the physiological and pathological state of the samples, the size of the study cohorts, and methodologic differences all contribute to the various outcomes in different studies, underscoring the challenges in biomarker identification and characterization by metabolomics, as is also the case in other ‘omics’ platforms. For this reason, it is unlikely that a single metabolite biomarker will be used to risk-stratify patients with PCa. A change in the global abundance profile of a subset of metabolites may be a more useful approach for screening, as has been suggested by McDunn et al[97]. The metabolite data may also have a more prognostic value when used in conjunction with genomic and proteomic markers that are better indicators of PCa aggressiveness.

(Ib) Characterization of the Prostate Cancer Metabolome by NMR Spectroscopy—Most NMR studies to date have been performed on prostate tissue biopsy samples and there are few studies on body fluids that have high sensitivity and can distinguish between patients with benign and metastatic PCa. A study[67] that compared prostatic fluid samples showed that the molar ratio of citrate: spermine is 5:1 in normal prostatic fluid, but a relatively higher level of spermine was found in prostatic fluid from men with PCa. Several studies have attempted to correlate the ratios of different metabolites in tissue extracts. Fowler et al[102] performed a study on a limited cohort of 7 patients with PCa and 13 with BPH. Statistically significant differences between the PCa and BPH groups were observed for the metabolite ratios of citrate, creatine, and phosphorylcholine to alanine, and citrate to glutamate. However, there was no correlation with Gleason grade for any of the ratios measured. Schiebler et al[21] compared metabolite abundance profiles in perchloric extracts of tissues from normal peripheral zone tissue, benign prostatic hyperplasia tissue, and adenocarcinoma from 13 patients. This study showed that in general citrate levels were significantly higher in glandular BPH tissue as compared to adenocarcinoma from the same patient. However citrate levels were lower in stromal BPH tissue and could not be used to discriminate between normal tissue and adenocarcinoma with certainty. A ^{31}P NMR study performed in 1993 by Cornel et al[24] showed that the ratios of phosphoethanolamine: total phosphate, phosphocholine: total phosphate, and glycerophosphoethanolamine: total phosphate were significantly different in tissue extracts from BPH and PCa patients. The data are consistent with *in vivo* MRS data that shows a change in tCho levels in men with PCa. Hahn et al[30] compared specimens of benign and malignant prostatic tissue from 50 patients using ^{1}H NMR on whole-tissue biopsy samples, but without MAS. They found that resonances from citrate, glutamate, and taurine from six spectral sub-regions when analyzed by multivariate analysis could discriminate between BPH and adenocarcinoma and gave good agreement with histopathology. Multivariate analysis was also deemed to be a more robust method as compared to analyzing intensity ratios of different metabolites. Swindle et al[29] determined that in addition to citrate and choline levels, lipid and lysine ratios (choline:citrate and lipid:lysine) were required to predict PCA with high accuracy (sensitivity and specificity). Similar to Hahn et al[30], they showed that pattern recognition methods are more reliable compared to metabolite ratios. It is evident that similar to the MS studies, multivariate statistical analysis of several metabolites such as hierarchical clustering analysis to generate heat maps may be necessary to risk-stratify patients with high accuracy.

A disadvantage of using tissue extracts is that there is more room for error due to metabolite losses during extraction and the efficiency of the extraction procedure used. High-resolution magic angle spinning (HR-MAS) NMR spectroscopy allows the quantitation of metabolites *ex vivo* without extraction, and more recent NMR studies[103,104,105,106,107] have utilized this approach for metabolic profiling and identification of new biomarkers. Cheng et al[108] have shown that the same tissue specimens can be used for NMR and pathology data. A drawback of HR-MAS is that it is not a high throughput method (although efforts are underway to automate data collection) and there is a need to standardize protocols to insure that the data is robust and reproducible. Data analysis is also more time consuming compared to NMR methods that use aqueous solutions. Several excellent reviews have been published on HR-MAS[109,110,111] and practical considerations for data collection and processing using HR-

MAS have also been published[88,112]. Nevertheless, HR-MAS is a powerful technique that can be used to extract quantitative information from peak intensities using standard one-dimensional (1D) NMR methods. Two dimensional correlation plots[113] that correlate two heteronuclei such as ^{1}H and ^{31}P or ^{1}H and ^{13}C can also be used to reduce spectral overlap and simplify the data[114,115]. Diffusion measurements using T_1 and T_2 relaxation times of the metabolites can also be measured and these can provide information about the rotational freedom and hence environment surrounding the metabolite in the tissue compartment[116]. HR-MAS studies have shown that the levels of spermine and citrate correlate well with the volume percentage of benign prostatic epithelial cells[108]. Phosphocholine, taurine, myo-inositol, lactate and alanine concentrations are higher in PCa compared to benign tissue. Therefore there is good correspondence between *ex vivo* studies using HR-MAS and *in vitro* studies using tissue extracts.

(II) Imaging the PCa metabolome

The identification of metabolite biomarkers that can distinguish between benign and metastatic PCa has clinical applications in diagnostic imaging of tumors. Current imaging techniques such as magnetic resonance imaging (MRI), X-ray computed tomography (CT), and ultrasonography do not report on the biochemical properties of the tumor, but are contrast techniques that measure tumor size and volume. The new field of “metabolic imaging” aims to detect cancer metabolic pathways using magnetic resonance spectroscopy imaging (MRSI) or hyperpolarized NMR methods to spatially map the metabolite signals in cancer tissues[20b]. Methods such as positron emission tomography (PET) already use such an approach in which metabolite tracers that are radiolabeled are monitored for their ability to accumulate in cancer tissue.^{18}F-fluoro-2-deoxyglucose (FDG)[18] and ^{11}C- or ^{18}F-labeled choline[117,118,119] can be used for PCa detection using PET imaging. Other metabolites that have been used with PET in breast, lung, colorectal and neuroendocrine tumors include the thymidine analog 3’-deoxy-3’-[^{18}F] fluorothymidine[120] which monitors cell division, the somastatin analog ^{68}Ga-DOTATOC[121], which binds the somastatin receptor 2, and 16-α-[^{18}F] fluoro-17-β-estradiol[122], which binds both estrogen receptor α and β. Although PET imaging is a very useful approach, the tracers are radioactive and there is limited information since PET techniques follow the steady state levels of only a single molecular tracer.

Magnetic resonance spectroscopic imaging (MRSI)[123,124] with an endorectal coil combines NMR spectroscopy with MRI techniques in that a subset of 2–3 tumor metabolites are visualized and that information is combined with information about tumor size and volume obtained from MRI. MRSI data is acquired on tumors by breaking down the visualized tissue into voxels that are typically 0.16 to 1 cm^3, and an NMR spectrum is taken in each voxel to quantify the abundance of 2–3 metabolites. By repeating this spatially across the tumor, one can map the metabolite abundance in both normal and PCa tissues across the prostate. This has the potential of providing molecular information about the tumor in a non-invasive fashion. As outlined in this review, the most common metabolite markers that have been associated with PCa are elevated choline and reduced citrate[124], although polyamines such as spermine, amino acids such as taurine, sarcosine, alanine, lysine, and lipids and creatnine have also been correlated. When MRSI was used to quantify the levels of citrate,

choline, and creatnine, and the ratio of {choline + creatnine}:citrate and citrate: normal citrate was spatially measured across the tumor, “definite cancer” was defined as voxels with (choline + creatnine) : citrate ratios > 0.86 and 3SD above normal[125] (Fig. 5). In this study[125], MRSI combined with MRI was reported to identify PCa with a very high sensitivity of 95% and specificity of 91%. The limitations of MRSI are obtaining good spectral and spatial resolution (limited to ~4 mm) in heterogeneous tissues such as the prostate, suppression of artifacts and development of robust software for data analysis and interpretation. In addition, only limited numbers of metabolites have so far been evaluated for metabolic imaging, and just the steady state abundance of these metabolites can be measured.

The use of hyperpolarized ^{13}C-labeled compounds in a perfusion MRI-based technique is a relatively new method that is used to image the accumulation of metabolites and their products in tumors[20b]. Hyperpolarized NMR allows for very high signal enhancements (of the order of 10^4–10^5 fold) as compared to nuclei at thermal equilibrium[126,127,128]. This method has great potential in overcoming the limited sensitivity of NMR in MRSI methods. The hyperpolarized state is generated in a molecular tracer by one of the three available methods: optical pumping and spin-exchange of noble gases[129,130], parahydrogen-induced polarization (PHIP)[131,132,133,134], or dynamic nuclear polarization (DNP)[134,133] before it is injected into the individual. The hyperpolarized state is very short-lived and the polarization decays to equilibrium with a time constant T_1. The relaxation time constant T_1 is an inherent property of NMR-active nuclei and nuclei such as ^{13}C have longer T_1 times than ^{1}H. The time available for imaging is 5–9 times the relaxation time T_1. The most widely used metabolite is [1-^{13}C]-pyruvate due to its pivotal role in cancer metabolism and its relatively long relaxation time T_1 of up to 60 s. The safety and feasibility of using [1-^{13}C]-pyruvate for metabolic imaging was demonstrated recently in the first clinical study in men[19]. When the metabolic flux of conversion of [1-^{13}C]-pyruvate to [1-^{13}C]-lactate was measured, the ratio of [1-^{13}C]-lactate/[1-^{13}C]-pyruvate was significantly elevated in regions of metastatic PCa compared to normal tissue. The flux of conversion of pyruvate to lactate was previously measured in a TRAMP mouse model and it correlated well with tumor grade[135]. Besides measuring the ratio of lactate to pyruvate, the change in signal can be measured over time and the data fit to kinetic models[136,137,90,138]. Several other metabolites and hyperpolarized nuclei (such as ^{29}Si, ^{6}Li, ^{89}Y)[139,140,141] are currently being tested for use due to their long T_1 relaxation times. Although hyperpolarized NMR based methods have a lot of potential, there are several constraints on its clinical application that need to be overcome. The biggest disadvantage of the technique is the short T_1 of most tracers that imposes constraints on the acquisition time. In addition, because of the low gyromagnetic ratio of ^{13}C and ^{15}N in comparison to ^{1}H, 16–100 fold more gradient power is required to achieve the same spatial resolution. New pulse sequences are also required for fast data collection of hyperpolarized nuclei. Other practical considerations include the safety of the metabolite tracer, the ability to rapidly generate hyperpolarized material, sterilize it and inject it into the host before the polarization decays.

Future Directions and Conclusions

In this review we have highlighted studies that have advanced our understanding of the prostate cancer metabolome. We described biomarkers that offer promise in distinguishing indolent from aggressive cancer and the development of new metabolic imaging techniques that could be highly beneficial for non-invasive diagnosis of metastatic PCa. There are several challenges to be overcome before metabolic profiling can become a valuable clinical tool to discriminate indolent from aggressive prostate cancer with high accuracy. It will be necessary to characterize as complete a metabolome as possible in large sample cohorts to verify and validate biomarkers. Integration of metabolic profiles with genomic or proteomic markers may be necessary to diagnose metastatic disease. The measurement of metabolic flux of metabolites in a particular pathway may be more insightful to determine PCa aggressiveness as compared to the steady state levels of the metabolites. The field of prostate cancer fluxomics is currently in its infancy. Another emerging field is pharmacometabolomics, i.e. the use of metabolic profiles for predicting drug treatment and therapy. Metabolic profiles could be useful not only in personalized medicine of PCa, but for also following patients before and after chemotherapy. These studies have the potential of providing new criteria to risk-stratify patients and develop novel approaches for individualized treatment.

Acknowledgements

We thank Drs. Thomas O'Connell (LipoScience, NC) and Andria Denmon (UC Irvine) for critical reading of the manuscript. Dr. Mark A Titus acknowledges support from Department of Defense (DOD) grant W81XWH-10-1-0273 and the University of Texas M.D. Anderson Cancer Center Support Grant CA016672.

References

1. Ercole CJ, Lange PH, Mathisen M, Chiou RK, Reddy PK, Vessella RL. Prostatic specific antigen and prostatic acid phosphatase in the monitoring and staging of patients with prostatic cancer. J Urol. 1987; 138(5):1181–1184. [PubMed: 2444720]
2. (a) Crawford ED. PSA testing: what is the use? Lancet. 2005; 365(9469):1447–1449. [PubMed: 15850617] (b) Wilson SS, Crawford ED. Screening for prostate cancer: current recommendations. Urol Clin North Am. 2004; 31(2):219–226. [PubMed: 15123402]
3. Catalona WJ, Smith DS, Ratliff TL, Dodds KM, Coplen DE, Yuan JJ, Petros JA, Andriole GL. Measurement of prostate-specific antigen in serum as a screening test for prostate cancer. N Engl J Med. 1991; 324(17):1156–1161. [PubMed: 1707140]
4. Catalona WJ, Partin AW, Slawin KM, Brawer MK, Flanigan RC, Patel A, Richie JP, deKernion JB, Walsh PC, Scardino PT, Lange PH, Subong EN, Parson RE, Gasior GH, Loveland KG, Southwick PC. Use of the percentage of free prostate-specific antigen to enhance differentiation of prostate cancer from benign prostatic disease: a prospective multicenter clinical trial. JAMA. 1998; 279(19): 1542–1547. [PubMed: 9605898]
5. Lilja H, Christensson A, Dahlen U, Matikainen MT, Nilsson O, Pettersson K, Lovgren T. Prostate-specific antigen in serum occurs predominantly in complex with alpha 1-antichymotrypsin. Clin Chem. 1991; 37(9):1618–1625. [PubMed: 1716536]
6. Partin AW, Brawer MK, Bartsch G, Horninger W, Taneja SS, Lepor H, Babaian R, Childs SJ, Stamey T, Fritsche HA, Sokoll L, Chan DW, Thiel RP, Cheli CD. Complexed prostate specific antigen improves specificity for prostate cancer detection: results of a prospective multicenter clinical trial. J Urol. 2003; 170(5):1787–1791. [PubMed: 14532777]

7. Heidenreich A. Identification of high-risk prostate cancer: role of prostate-specific antigen, PSA doubling time, and PSA velocity. Eur Urol. 2008; 54(5):976–977. discussion 978–9. [PubMed: 18640768]

8. Prensner JR, Rubin MA, Wei JT, Chinnaiyan AM. Beyond PSA: the next generation of prostate cancer biomarkers. Sci Transl Med. 2012; 4(127):127rv3.

9. Bussemakers MJ, van Bokhoven A, Verhaegh GW, Smit FP, Karthaus HF, Schalken JA, Debruyne FM, Ru N, Isaacs WB. DD3: a new prostate-specific gene, highly overexpressed in prostate cancer. Cancer Res. 1999; 59(23):5975–5979. [PubMed: 10606244]

10. de Kok JB, Verhaegh GW, Roelofs RW, Hessels D, Kiemeney LA, Aalders TW, Swinkels DW, Schalken JA. DD3(PCA3), a very sensitive and specific marker to detect prostate tumors. Cancer Res. 2002; 62(9):2695–2698. [PubMed: 11980670]

11. Prensner JR, Chinnaiyan AM. Oncogenic gene fusions in epithelial carcinomas. Curr Opin Genet Dev. 2009; 19(1):82–91. [PubMed: 19233641]

12. (a) Rubin MA, Zhou M, Dhanasekaran SM, Varambally S, Barrette TR, Sanda MG, Pienta KJ, Ghosh D, Chinnaiyan AM. alpha-Methylacyl coenzyme A racemase as a tissue biomarker for prostate cancer. JAMA. 2002; 287(13):1662–1670. [PubMed: 11926890] (b) Rubin MA, Bismar TA, Andren O, Mucci L, Kim R, Shen R, Ghosh D, Wei JT, Chinnaiyan AM, Adami HO, Kantoff PW, Johansson JE. Decreased alpha-methylacyl CoA racemase expression in localized prostate cancer is associated with an increased rate of biochemical recurrence and cancer-specific death. Cancer Epidemiol Biomarkers Prev. 2005; 14(6):1424–1432. [PubMed: 15941951]

13. Attard G, Swennenhuis JF, Olmos D, Reid AH, Vickers E, A'Hern R, Levink R, Coumans F, Moreira J, Riisnaes R, Oommen NB, Hawche G, Jameson C, Thompson E, Sipkema R, Carden CP, Parker C, Dearnaley D, Kaye SB, Cooper CS, Molina A, Cox ME, Terstappen LW, de Bono JS. Characterization of ERG, AR and PTEN gene status in circulating tumor cells from patients with castration-resistant prostate cancer. Cancer Res. 2009; 69(7):2912–2918. [PubMed: 19339269]

14. Duijvesz D, Luider T, Bangma CH, Jenster G. Exosomes as biomarker treasure chests for prostate cancer. Eur Urol. 2011; 59(5):823–831. [PubMed: 21196075]

15. Hessels D, Schalken JA. The use of PCA3 in the diagnosis of prostate cancer. Nat Rev Urol. 2009; 6(5):255–261. [PubMed: 19424173]

16. Roobol MJ, Schroder FH, van Leeuwen P, Wolters T, van den Bergh RC, van Leenders GJ, Hessels D. Performance of the prostate cancer antigen 3 (PCA3) gene and prostate-specific antigen in prescreened men: exploring the value of PCA3 for a first-line diagnostic test. Eur Urol. 2010; 58(4):475–481. [PubMed: 20637539]

17. Haese A, de la Taille A, van Poppel H, Marberger M, Stenzl A, Mulders PF, Huland H, Abbou CC, Remzi M, Tinzl M, Feyerabend S, Stillebroer AB, van Gils MP, Schalken JA. Clinical utility of the PCA3 urine assay in European men scheduled for repeat biopsy. Eur Urol. 2008; 54(5):1081–1088. [PubMed: 18602209]

18. Blodgett TM, Meltzer CC, Townsend DW. PET/CT: form and function. Radiology. 2007; 242(2): 360–385. [PubMed: 17255408]

19. Nelson SJ, Kurhanewicz J, Vigneron DB, Larson PE, Harzstark AL, Ferrone M, van Criekinge M, Chang JW, Bok R, Park I, Reed G, Carvajal L, Small EJ, Munster P, Weinberg VK, Ardenkjaer-Larsen JH, Chen AP, Hurd RE, Odegardstuen LI, Robb FJ, Tropp J, Murray JA. Metabolic imaging of patients with prostate cancer using hyperpolarized [1-(1)(3)C]pyruvate. Sci Transl Med. 2013; 5(198):198ra108.

20. (a) Gulley JL, Emberton M, Kurhanewicz J, Choyke P. Progress in prostate cancer imaging. Urol Oncol. 2012; 30(6):938–939. [PubMed: 23218070] (b) Kurhanewicz J, Vigneron DB, Brindle K, Chekmenev EY, Comment A, Cunningham CH, Deberardinis RJ, Green GG, Leach MO, Rajan SS, Rizi RR, Ross BD, Warren WS, Malloy CR. Analysis of cancer metabolism by imaging hyperpolarized nuclei: prospects for translation to clinical research. Neoplasia. 2011; 13(2):81–97. [PubMed: 21403835]

21. Schiebler ML, Miyamoto KK, White M, Maygarden SJ, Mohler JL. In vitro high resolution 1H-spectroscopy of the human prostate: benign prostatic hyperplasia, normal peripheral zone and adenocarcinoma. Magn Reson Med. 1993; 29(3):285–291. [PubMed: 7680746]

22. Sillerud LO, Halliday KR, Griffey RH, Fenoglio-Preiser C, Sheppard S. In vivo 13C NMR spectroscopy of the human prostate. Magn Reson Med. 1988; 8(2):224–230. [PubMed: 2463457]
23. Halliday KR, Fenoglio-Preiser C, Sillerud LO. Differentiation of human tumors from nonmalignant tissue by natural-abundance 13C NMR spectroscopy. Magn Reson Med. 1988; 7(4): 384–411. [PubMed: 2459580]
24. Cornel EB, Smits GA, Oosterhof GO, Karthaus HF, Deburyne FM, Schalken JA, Heerschap A. Characterization of human prostate cancer, benign prostatic hyperplasia and normal prostate by in vitro 1H and 31P magnetic resonance spectroscopy. J Urol. 1993; 150(6):2019–2024. [PubMed: 7693985]
25. Averna TA, Kline EE, Smith AY, Sillerud LO. A decrease in 1H nuclear magnetic resonance spectroscopically determined citrate in human seminal fluid accompanies the development of prostate adenocarcinoma. J Urol. 2005; 173(2):433–438. [PubMed: 15643195]
26. Kline EE, Treat EG, Averna TA, Davis MS, Smith AY, Sillerud LO. Citrate concentrations in human seminal fluid and expressed prostatic fluid determined via 1H nuclear magnetic resonance spectroscopy outperform prostate specific antigen in prostate cancer detection. J Urol. 2006; 176(5):2274–2279. [PubMed: 17070311]
27. Serkova NJ, Gamito EJ, Jones RH, O'Donnell C, Brown JL, Green S, Sullivan H, Hedlund T, Crawford ED. The metabolites citrate, myo-inositol, and spermine are potential age-independent markers of prostate cancer in human expressed prostatic secretions. Prostate. 2008; 68(6):620–628. [PubMed: 18213632]
28. Swindle P, Ramadan S, Stanwell P, McCredie S, Russell P, Mountford C. Proton magnetic resonance spectroscopy of the central, transition and peripheral zones of the prostate: assignments and correlation with histopathology. MAGMA. 2008; 21(6):423–434. [PubMed: 18797949]
29. Swindle P, McCredie S, Russell P, Himmelreich U, Khadra M, Lean C, Mountford C. Pathologic characterization of human prostate tissue with proton MR spectroscopy. Radiology. 2003; 228(1): 144–151. [PubMed: 12832578]
30. Hahn P, Smith IC, Leboldus L, Littman C, Somorjai RL, Bezabeh T. The classification of benign and malignant human prostate tissue by multivariate analysis of 1H magnetic resonance spectra. Cancer Res. 1997; 57(16):3398–3401. [PubMed: 9270004]
31. Sreekumar A, Poisson LM, Rajendiran TM, Khan AP, Cao Q, Yu J, Laxman B, Mehra R, Lonigro RJ, Li Y, Nyati MK, Ahsan A, Kalyana-Sundaram S, Han B, Cao X, Byun J, Omenn GS, Ghosh D, Pennathur S, Alexander DC, Berger A, Shuster JR, Wei JT, Varambally S, Beecher C, Chinnaiyan AM. Metabolomic profiles delineate potential role for sarcosine in prostate cancer progression. Nature. 2009; 457(7231):910–914. [PubMed: 19212411]
32. Warburg O. On the origin of cancer cells. Science. 1956; 123(3191):309–314. [PubMed: 13298683]
33. Warburg O. On respiratory impairment in cancer cells. Science. 1956; 124(3215):269–270. [PubMed: 13351639]
34. Hensley CT, Wasti AT, DeBerardinis RJ. Glutamine and cancer: cell biology, physiology, and clinical opportunities. J Clin Invest. 2013; 123(9):3678–3684. [PubMed: 23999442]
35. DeBerardinis RJ, Cheng T. Q's next: the diverse functions of glutamine in metabolism, cell biology and cancer. Oncogene. 2010; 29(3):313–324. [PubMed: 19881548]
36. Swinnen JV, Brusselmans K, Verhoeven G. Increased lipogenesis in cancer cells: new players, novel targets. Curr Opin Clin Nutr Metab Care. 2006; 9(4):358–365. [PubMed: 16778563]
37. Massie CE, Lynch A, Ramos-Montoya A, Boren J, Stark R, Fazli L, Warren A, Scott H, Madhu B, Sharma N, Bon H, Zecchini V, Smith DM, Denicola GM, Mathews N, Osborne M, Hadfield J, Macarthur S, Adryan B, Lyons SK, Brindle KM, Griffiths J, Gleave ME, Rennie PS, Neal DE, Mills IG. The androgen receptor fuels prostate cancer by regulating central metabolism and biosynthesis. EMBO J. 2011; 30(13):2719–2733. [PubMed: 21602788]
38. Jones RG, Thompson CB. Tumor suppressors and cell metabolism: a recipe for cancer growth. Genes Dev. 2009; 23(5):537–548. [PubMed: 19270154]
39. DeBerardinis RJ, Lum JJ, Hatzivassiliou G, Thompson CB. The biology of cancer: metabolic reprogramming fuels cell growth and proliferation. Cell Metab. 2008; 7(1):11–20. [PubMed: 18177721]

40. Semenza GL. HIF-1: upstream and downstream of cancer metabolism. Curr Opin Genet Dev. 2010; 20(1):51–56. [PubMed: 19942427]

41. Semenza GL. Defining the role of hypoxia-inducible factor 1 in cancer biology and therapeutics. Oncogene. 2010; 29(5):625–634. [PubMed: 19946328]

42. Hanahan D, Weinberg RA. Hallmarks of cancer: the next generation. Cell. 2011; 144(5):646–674. [PubMed: 21376230]

43. DeBerardinis RJ, Thompson CB. Cellular metabolism and disease: what do metabolic outliers teach us? Cell. 2012; 148(6):1132–1144. [PubMed: 22424225]

44. Parsons DW, Jones S, Zhang X, Lin JC, Leary RJ, Angenendt P, Mankoo P, Carter H, Siu IM, Gallia GL, Olivi A, McLendon R, Rasheed BA, Keir S, Nikolskaya T, Nikolsky Y, Busam DA, Tekleab H, Diaz LA Jr, Hartigan J, Smith DR, Strausberg RL, Marie SK, Shinjo SM, Yan H, Riggins GJ, Bigner DD, Karchin R, Papadopoulos N, Parmigiani G, Vogelstein B, Velculescu VE, Kinzler KW. An integrated genomic analysis of human glioblastoma multiforme. Science. 2008; 321(5897):1807–1812. [PubMed: 18772396]

45. Yan H, Parsons DW, Jin G, McLendon R, Rasheed BA, Yuan W, Kos I, Batinic-Haberle I, Jones S, Riggins GJ, Friedman H, Friedman A, Reardon D, Herndon J, Kinzler KW, Velculescu VE, Vogelstein B, Bigner DD. IDH1 and IDH2 mutations in gliomas. N Engl J Med. 2009; 360(8): 765–773. [PubMed: 19228619]

46. Figueroa ME, Abdel-Wahab O, Lu C, Ward PS, Patel J, Shih A, Li Y, Bhagwat N, Vasanthakumar A, Fernandez HF, Tallman MS, Sun Z, Wolniak K, Peeters JK, Liu W, Choe SE, Fantin VR, Paietta E, Lowenberg B, Licht JD, Godley LA, Delwel R, Valk PJ, Thompson CB, Levine RL, Melnick A. Leukemic IDH1 and IDH2 mutations result in a hypermethylation phenotype, disrupt TET2 function, and impair hematopoietic differentiation. Cancer Cell. 2010; 18(6):553–567. [PubMed: 21130701]

47. Xu W, Yang H, Liu Y, Yang Y, Wang P, Kim SH, Ito S, Yang C, Xiao MT, Liu LX, Jiang WQ, Liu J, Zhang JY, Wang B, Frye S, Zhang Y, Xu YH, Lei QY, Guan KL, Zhao SM, Xiong Y. Oncometabolite 2-hydroxyglutarate is a competitive inhibitor of alpha-ketoglutarate-dependent dioxygenases. Cancer Cell. 2011; 19(1):17–30. [PubMed: 21251613]

48. Dang L, White DW, Gross S, Bennett BD, Bittinger MA, Driggers EM, Fantin VR, Jang HG, Jin S, Keenan MC, Marks KM, Prins RM, Ward PS, Yen KE, Liau LM, Rabinowitz JD, Cantley LC, Thompson CB, Vander Heiden MG, Su SM. Cancer-associated IDH1 mutations produce 2-hydroxyglutarate. Nature. 2009; 462(7274):739–744. [PubMed: 19935646]

49. Lu C, Venneti S, Akalin A, Fang F, Ward PS, Dematteo RG, Intlekofer AM, Chen C, Ye J, Hameed M, Nafa K, Agaram NP, Cross JR, Khanin R, Mason CE, Healey JH, Lowe SW, Schwartz GK, Melnick A, Thompson CB. Induction of sarcomas by mutant IDH2. Genes Dev. 2013; 27(18):1986–1998. [PubMed: 24065766]

50. Baysal BE, Ferrell RE, Willett-Brozick JE, Lawrence EC, Myssiorek D, Bosch A, van der Mey A, Taschner PE, Rubinstein WS, Myers EN, Richard CW 3rd, Cornelisse CJ, Devilee P, Devlin B. Mutations in SDHD, a mitochondrial complex II gene, in hereditary paraganglioma. Science. 2000; 287(5454):848–851. [PubMed: 10657297]

51. Burnichon N, Briere JJ, Libe R, Vescovo L, Riviere J, Tissier F, Jouanno E, Jeunemaitre X, Benit P, Tzagoloff A, Rustin P, Bertherat J, Favier J, Gimenez-Roqueplo AP. SDHA is a tumor suppressor gene causing paraganglioma. Hum Mol Genet. 2010; 19(15):3011–3020. [PubMed: 20484225]

52. Tomlinson IP, Alam NA, Rowan AJ, Barclay E, Jaeger EE, Kelsell D, Leigh I, Gorman P, Lamlum H, Rahman S, Roylance RR, Olpin S, Bevan S, Barker K, Hearle N, Houlston RS, Kiuru M, Lehtonen R, Karhu A, Vilkki S, Laiho P, Eklund C, Vierimaa O, Aittomaki K, Hietala M, Sistonen P, Paetau A, Salovaara R, Herva R, Launonen V, Aaltonen LA. Germline mutations in FH predispose to dominantly inherited uterine fibroids, skin leiomyomata and papillary renal cell cancer. Nat Genet. 2002; 30(4):406–410. [PubMed: 11865300]

53. Tong WH, Sourbier C, Kovtunovych G, Jeong SY, Vira M, Ghosh M, Romero VV, Sougrat R, Vaulont S, Viollet B, Kim YS, Lee S, Trepel J, Srinivasan R, Bratslavsky G, Yang Y, Linehan WM, Rouault TA. The glycolytic shift in fumarate-hydratase-deficient kidney cancer lowers AMPK levels, increases anabolic propensities and lowers cellular iron levels. Cancer Cell. 2011; 20(3):315–327. [PubMed: 21907923]

54. Finley LW, Zhang J, Ye J, Ward PS, Thompson CB. SnapShot: cancer metabolism pathways. Cell Metab. 2013; 17(3):466–466. e2. [PubMed: 23473039]
55. Kaplon J, Zheng L, Meissl K, Chaneton B, Selivanov VA, Mackay G, van der Burg SH, Verdegaal EM, Cascante M, Shlomi T, Gottlieb E, Peeper DS. A key role for mitochondrial gatekeeper pyruvate dehydrogenase in oncogene-induced senescence. Nature. 2013; 498(7452):109–112. [PubMed: 23685455]
56. Takahashi H, McCaffery JM, Irizarry RA, Boeke JD. Nucleocytosolic acetyl-coenzyme a synthetase is required for histone acetylation and global transcription. Mol Cell. 2006; 23(2):207–217. [PubMed: 16857587]
57. Wellen KE, Hatzivassiliou G, Sachdeva UM, Bui TV, Cross JR, Thompson CB. ATP-citrate lyase links cellular metabolism to histone acetylation. Science. 2009; 324(5930):1076–1080. [PubMed: 19461003]
58. McNeal JE, Redwine EA, Freiha FS, Stamey TA. Zonal distribution of prostatic adenocarcinoma. Correlation with histologic pattern and direction of spread. Am J Surg Pathol. 1988; 12(12):897–906. [PubMed: 3202246]
59. Huggins C, Scott WW, Heinen JH. Chemical composition of human semen and of the secretions of the prostate and seminal vesicles. Am J Physiol. 1942; 136:467–473.
60. White KY, Rodemich L, Nyalwidhe JO, Comunale MA, Clements MA, Lance RS, Schellhammer PF, Mehta AS, Semmes OJ, Drake RR. Glycomic characterization of prostate-specific antigen and prostatic acid phosphatase in prostate cancer and benign disease seminal plasma fluids. J Proteome Res. 2009; 8(2):620–630. [PubMed: 19128049]
61. Costello LC, Franklin RB. Concepts of citrate production and secretion by prostate. 1. Metabolic relationships. Prostate. 1991; 18(1):25–46. [PubMed: 1987578]
62. Franklin, RB.; Costello, LC. Intermediary energy metabolism of normal and malignant prostate epithelial cells. In: Naz, RK., editor. Prostate: Basic and Clinical aspects. New York: CRC Press; 1997. p. 115-150.
63. Costello LC, Franklin RB. The intermediary metabolism of the prostate: a key to understanding the pathogenesis and progression of prostate malignancy. Oncology. 2000; 59(4):269–282. [PubMed: 11096338]
64. Costello LC, Franklin RB, Feng P. Mitochondrial function, zinc, and intermediary metabolism relationships in normal prostate and prostate cancer. Mitochondrion. 2005; 5(3):143–153. [PubMed: 16050980]
65. Marberger H, Marberger E, Mann T, Lutwak-Mann C. Citric acid in human prostatic secretion and metastasizing cancer of prostate gland. Br Med J. 1962; 1(5281):835–836. [PubMed: 14469565]
66. Kolenko V, Teper E, Kutikov A, Uzzo R. Zinc and zinc transporters in prostate carcinogenesis. Nat Rev Urol. 2013; 10(4):219–226. [PubMed: 23478540]
67. Lynch MJ, Nicholson JK. Proton MRS of human prostatic fluid: correlations between citrate, spermine, and myo-inositol levels and changes with disease. Prostate. 1997; 30(4):248–255. [PubMed: 9111602]
68. Glunde K, Jacobs MA, Bhujwalla ZM. Choline metabolism in cancer: implications for diagnosis and therapy. Expert Rev Mol Diagn. 2006; 6(6):821–829. [PubMed: 17140369]
69. (a) Muller SA, Holzapfel K, Seidl C, Treiber U, Krause BJ, Senekowitsch-Schmidtke R. Characterization of choline uptake in prostate cancer cells following bicalutamide and docetaxel treatment. Eur J Nucl Med Mol Imaging. 2009; 36(9):1434–1442. [PubMed: 19352653] (b) Keshari KR, Tsachres H, Iman R, Delos Santos L, Tabatabai ZL, Shinohara K, Vigneron DB, Kurhanewicz J. Correlation of phospholipid metabolites with prostate cancer pathologic grade, proliferative status and surgical stage - impact of tissue environment. NMR Biomed. 2011; 24(6): 691–699. [PubMed: 21793074]
70. Milkevitch M, Shim H, Pilatus U, Pickup S, Wehrle JP, Samid D, Poptani H, Glickson JD, Delikatny EJ. Increases in NMR-visible lipid and glycerophosphocholine during phenylbutyrate-induced apoptosis in human prostate cancer cells. Biochim Biophys Acta. 2005; 1734(1):1–12. [PubMed: 15866478]

71. Glunde K, Shah T, Winnard PT Jr, Raman V, Takagi T, Vesuna F, Artemov D, Bhujwalla ZM. Hypoxia regulates choline kinase expression through hypoxia-inducible factor-1 alpha signaling in a human prostate cancer model. Cancer Res. 2008; 68(1):172–180. [PubMed: 18172309]

72. Stenman K, Hauksson JB, Grobner G, Stattin P, Bergh A, Riklund K. Detection of polyunsaturated omega-6 fatty acid in human malignant prostate tissue by 1D and 2D high-resolution magic angle spinning NMR spectroscopy. MAGMA. 2009; 22(6):327–331. [PubMed: 19921294]

73. Huggins C, Hodges CV. Studies on prostatic cancer: I. The effect of castration, of estrogen and of androgen injection on serum phosphatases in metastatic carcinoma of the prostate. 1941. J Urol. 2002; 168(1):9–12. [PubMed: 12050481]

74. Huggins C. Endocrine-induced regression of cancers. Am J Surg. 1978; 136(2):233–238. [PubMed: 150802]

75. Tomkins GM. The enzymatic reduction of delta 4-3-ketosteroids. J Biol Chem. 1957; 225(1):13–24. [PubMed: 13416214]

76. Silver RI, Wiley EL, Davis DL, Thigpen AE, Russell DW, McConnell JD. Expression and regulation of steroid 5 alpha-reductase 2 in prostate disease. J Urol. 1994; 152(2 Pt 1):433–437. [PubMed: 7516976]

77. Andersson S, Bishop RW, Russell DW. Expression cloning and regulation of steroid 5 alpha-reductase, an enzyme essential for male sexual differentiation. J Biol Chem. 1989; 264(27):16249–16255. [PubMed: 2476440]

78. Bruchovsky N, Wilson JD. The conversion of testosterone to 5-alpha-androstan-17-beta-ol-3-one by rat prostate in vivo and in vitro. J Biol Chem. 1968; 243(8):2012–2021. [PubMed: 4384673]

79. Geller J, Albert J, Loza D, Geller S, Stoeltzing W, de la Vega D. DHT concentrations in human prostate cancer tissue. J Clin Endocrinol Metab. 1978; 46(3):440–444. [PubMed: 87401]

80. Lubahn DB, Joseph DR, Sullivan PM, Willard HF, French FS, Wilson EM. Cloning of human androgen receptor complementary DNA and localization to the X chromosome. Science. 1988; 240(4850):327–330. [PubMed: 3353727]

81. Chang CS, Kokontis J, Liao ST. Molecular cloning of human and rat complementary DNA encoding androgen receptors. Science. 1988; 240(4850):324–326. [PubMed: 3353726]

82. Tilley WD, Marcelli M, Wilson JD, McPhaul MJ. Characterization and expression of a cDNA encoding the human androgen receptor. Proc Natl Acad Sci U S A. 1989; 86(1):327–331. [PubMed: 2911578]

83. Logothetis CJ, Gallick GE, Maity SN, Kim J, Aparicio A, Efstathiou E, Lin SH. Molecular classification of prostate cancer progression: foundation for marker-driven treatment of prostate cancer. Cancer Discov. 2013; 3(8):849–861. [PubMed: 23811619]

84. Thysell E, Surowiec I, Hornberg E, Crnalic S, Widmark A, Johansson AI, Stattin P, Bergh A, Moritz T, Antti H, Wikstrom P. Metabolomic characterization of human prostate cancer bone metastases reveals increased levels of cholesterol. PLoS One. 2010; 5(12):e14175. [PubMed: 21151972]

85. Whiley L, Legido-Quigley C. Current strategies in the discovery of small-molecule biomarkers for Alzheimer's disease. Bioanalysis. 2011; 3(10):1121–1142. [PubMed: 21585307]

86. Dunn WB, Bailey NJ, Johnson HE. Measuring the metabolome: current analytical technologies. Analyst. 2005; 130(5):606–625. [PubMed: 15852128]

87. (a) Zhang A, Sun H, Wang P, Han Y, Wang X. Modern analytical techniques in metabolomics analysis. Analyst. 2012; 137(2):293–300. [PubMed: 22102985] (b) Dunn WB, Broadhurst DI, Atherton HJ, Goodacre R, Griffin JL. Systems level studies of mammalian metabolomes: the roles of mass spectrometry and nuclear magnetic resonance spectroscopy. Chem Soc Rev. 2011; 40(1): 387–426. [PubMed: 20717559]

88. Beckonert O, Coen M, Keun HC, Wang Y, Ebbels TM, Holmes E, Lindon JC, Nicholson JK. High-resolution magic-angle-spinning NMR spectroscopy for metabolic profiling of intact tissues. Nat Protoc. 2010; 5(6):1019–1032. [PubMed: 20539278]

89. Harrison C, Yang C, Jindal A, DeBerardinis RJ, Hooshyar MA, Merritt M, Dean Sherry A, Malloy CR. Comparison of kinetic models for analysis of pyruvate-to-lactate exchange by hyperpolarized 13 C NMR. NMR Biomed. 2012; 25(11):1286–1294. [PubMed: 22451442]

90. Keshari KR, Kurhanewicz J, Jeffries RE, Wilson DM, Dewar BJ, Van Criekinge M, Zierhut M, Vigneron DB, Macdonald JM. Hyperpolarized (13)C spectroscopy and an NMR-compatible bioreactor system for the investigation of real-time cellular metabolism. Magn Reson Med. 2010; 63(2):322–329. [PubMed: 20099325]
91. Merritt ME, Harrison C, Storey C, Jeffrey FM, Sherry AD, Malloy CR. Hyperpolarized 13C allows a direct measure of flux through a single enzyme-catalyzed step by NMR. Proc Natl Acad Sci U S A. 2007; 104(50):19773–19777. [PubMed: 18056642]
92. Witney TH, Brindle KM. Imaging tumour cell metabolism using hyperpolarized 13C magnetic resonance spectroscopy. Biochem Soc Trans. 2010; 38(5):1220–1224. [PubMed: 20863288]
93. Swisher CL, Larson PE, Kruttwig K, Kerr AB, Hu S, Bok RA, Goga A, Pauly JM, Nelson SJ, Kurhanewicz J, Vigneron DB. Quantitative measurement of cancer metabolism using stimulated echo hyperpolarized carbon-13 MRS. Magn Reson Med. 2013
94. Jentzmik F, Stephan C, Lein M, Miller K, Kamlage B, Bethan B, Kristiansen G, Jung K. Sarcosine in prostate cancer tissue is not a differential metabolite for prostate cancer aggressiveness and biochemical progression. J Urol. 2011; 185(2):706–711. [PubMed: 21168877]
95. Jentzmik F, Stephan C, Miller K, Schrader M, Erbersdobler A, Kristiansen G, Lein M, Jung K. Sarcosine in urine after digital rectal examination fails as a marker in prostate cancer detection and identification of aggressive tumours. Eur Urol. 2010; 58(1):12–18. discussion 20–1. [PubMed: 20117878]
96. Cao DL, Ye DW, Zhu Y, Zhang HL, Wang YX, Yao XD. Efforts to resolve the contradictions in early diagnosis of prostate cancer: a comparison of different algorithms of sarcosine in urine. Prostate Cancer Prostatic Dis. 2011; 14(2):166–172. [PubMed: 21321584]
97. McDunn JE, Li Z, Adam KP, Neri BP, Wolfert RL, Milburn MV, Lotan Y, Wheeler TM. Metabolomic signatures of aggressive prostate cancer. Prostate. 2013; 73(14):1547–1560. [PubMed: 23824564]
98. Schaffner CP. Prostatic cholesterol metabolism: regulation and alteration. Prog Clin Biol Res. 1981; 75A:279–324. [PubMed: 6175978]
99. Soccio RE, Breslow JL. Intracellular cholesterol transport. Arterioscler Thromb Vasc Biol. 2004; 24(7):1150–1160. [PubMed: 15130918]
100. Crnalic S, Hornberg E, Wikstrom P, Lerner UH, Tieva A, Svensson O, Widmark A, Bergh A. Nuclear androgen receptor staining in bone metastases is related to a poor outcome in prostate cancer patients. Endocr Relat Cancer. 2010; 17(4):885–895. [PubMed: 20688881]
101. Jernberg E, Thysell E, Bovinder Ylitalo E, Rudolfsson S, Crnalic S, Widmark A, Bergh A, Wikstrom P. Characterization of prostate cancer bone metastases according to expression levels of steroidogenic enzymes and androgen receptor splice variants. PLoS One. 2013; 8(11):e77407. [PubMed: 24244276]
102. Fowler AH, Pappas AA, Holder JC, Finkbeiner AE, Dalrymple GV, Mullins MS, Sprigg JR, Komoroski RA. Differentiation of human prostate cancer from benign hypertrophy by in vitro 1H NMR. Magn Reson Med. 1992; 25(1):140–147. [PubMed: 1375702]
103. Tomlins AM, Foxall PJD, Lindon JC, Nicholson JK, Lynch MJ, Spraul M, Everett JR. High resolution magic angle spinning 1H nuclear magnetic resonance analysis of intact prostatic hyperplastic and tumour tissues. Anal. Commun. 1998; 35:113–115.
104. Burns MA, He W, Wu CL, Cheng LL. Quantitative pathology in tissue MR spectroscopy based human prostate metabolomics. Technol Cancer Res Treat. 2004; 3(6):591–598. [PubMed: 15560717]
105. Ratiney H, Albers MJ, Rabeson H, Kurhanewicz J. Semi-parametric time-domain quantification of HR-MAS data from prostate tissue. NMR Biomed. 2010; 23(10):1146–1157. [PubMed: 20842756]
106. Levin YS, Albers MJ, Butler TN, Spielman D, Peehl DM, Kurhanewicz J. Methods for metabolic evaluation of prostate cancer cells using proton and (13)C HR-MAS spectroscopy and [3-(13)C] pyruvate as a metabolic substrate. Magn Reson Med. 2009; 62(5):1091–1098. [PubMed: 19780158]

107. Cheng LL, Burns MA, Taylor JL, He W, Halpern EF, McDougal WS, Wu CL. Metabolic characterization of human prostate cancer with tissue magnetic resonance spectroscopy. Cancer Res. 2005; 65(8):3030–3034. [PubMed: 15833828]

108. Cheng LL, Wu C, Smith MR, Gonzalez RG. Non-destructive quantitation of spermine in human prostate tissue samples using HRMAS 1H NMR spectroscopy at 9.4 T. FEBS Lett. 2001; 494(1–2):112–116. [PubMed: 11297745]

109. Decelle EA, Cheng LL. High-resolution magic angle spinning H MRS in prostate cancer. NMR Biomed. 2013

110. Lindon JC, Beckonert O, Holmes E, Nicholson JK. High-resolution magic angle spinning NMR spectroscopy: application to biomedical studies. Prog. Nuc. Magn. Reson. Spectr. 2009; 55:79–100.

111. DeFeo EM, Cheng LL. Characterizing human cancer metabolomics with ex vivo 1H HRMAS MRS. Technol Cancer Res Treat. 2010; 9(4):381–391. [PubMed: 20626203]

112. Swanson MG, Zektzer AS, Tabatabai ZL, Simko J, Jarso S, Keshari KR, Schmitt L, Carroll PR, Shinohara K, Vigneron DB, Kurhanewicz J. Quantitative analysis of prostate metabolites using 1H HR-MAS spectroscopy. Magn Reson Med. 2006; 55(6):1257–1264. [PubMed: 16685733]

113. Swanson MG, Keshari KR, Tabatabai ZL, Simko JP, Shinohara K, Carroll PR, Zektzer AS, Kurhanewicz J. Quantification of choline- and ethanolamine-containing metabolites in human prostate tissues using 1H HR-MAS total correlation spectroscopy. Magn Reson Med. 2008; 60(1):33–40. [PubMed: 18581409]

114. Soubias O, Piotto M, Saurel O, Assemat O, Reat V, Milon A. Detection of natural abundance 1H-13C correlations of cholesterol in its membrane environment using a gradient enhanced HSQC experiment under high resolution magic angle spinning. J Magn Reson. 2003; 165(2): 303–308. [PubMed: 14643713]

115. Wang Y, Cloarec O, Tang H, Lindon JC, Holmes E, Kochhar S, Nicholson JK. Magic angle spinning NMR and 1H-31P heteronuclear statistical total correlation spectroscopy of intact human gut biopsies. Anal Chem. 2008; 80(4):1058–1066. [PubMed: 18205334]

116. Griffin JL, Troke J, Walker LA, Shore RF, Lindon JC, Nicholson JK. The biochemical profile of rat testicular tissue as measured by magic angle spinning 1H NMR spectroscopy. FEBS Lett. 2000; 486(3):225–229. [PubMed: 11119708]

117. Breeuwsma AJ, Pruim J, van den Bergh AC, Leliveld AM, Nijman RJ, Dierckx RA, de Jong IJ. Detection of local, regional, and distant recurrence in patients with psa relapse after external-beam radiotherapy using (11)C-choline positron emission tomography. Int J Radiat Oncol Biol Phys. 2010; 77(1):160–164. [PubMed: 19783375]

118. Piert M, Park H, Khan A, Siddiqui J, Hussain H, Chenevert T, Wood D, Johnson T, Shah RB, Meyer C. Detection of aggressive primary prostate cancer with 11C-choline PET/CT using multimodality fusion techniques. J Nucl Med. 2009; 50(10):1585–1593. [PubMed: 19759109]

119. Talbot JN, Gutman F, Fartoux L, Grange JD, Ganne N, Kerrou K, Grahek D, Montravers F, Poupon R, Rosmorduc O. PET/CT in patients with hepatocellular carcinoma using [(18)F]fluorocholine: preliminary comparison with [(18)F]FDG PET/CT. Eur J Nucl Med Mol Imaging. 2006; 33(11):1285–1289. [PubMed: 16802155]

120. Buck AK, Herrmann K, Shen C, Dechow T, Schwaiger M, Wester HJ. Molecular imaging of proliferation in vivo: positron emission tomography with [18F]fluorothymidine. Methods. 2009; 48(2):205–215. [PubMed: 19318128]

121. Buchmann I, Henze M, Engelbrecht S, Eisenhut M, Runz A, Schafer M, Schilling T, Haufe S, Herrmann T, Haberkorn U. Comparison of 68Ga-DOTATOC PET and 111In-DTPAOC (Octreoscan) SPECT in patients with neuroendocrine tumours. Eur J Nucl Med Mol Imaging. 2007; 34(10):1617–1626. [PubMed: 17520251]

122. Mortimer JE, Dehdashti F, Siegel BA, Katzenellenbogen JA, Fracasso P, Welch MJ. Positron emission tomography with 2-[18F]Fluoro-2-deoxy-D-glucose and 16alpha-[18F]fluoro-17beta-estradiol in breast cancer: correlation with estrogen receptor status and response to systemic therapy. Clin Cancer Res. 1996; 2(6):933–939. [PubMed: 9816253]

123. Chuang CF, Chan AA, Larson D, Verhey LJ, McDermott M, Nelson SJ, Pirzkall A. Potential value of MR spectroscopic imaging for the radiosurgical management of patients with recurrent high-grade gliomas. Technol Cancer Res Treat. 2007; 6(5):375–382. [PubMed: 17877425]

124. Kurhanewicz J, Vigneron DB. Advances in MR spectroscopy of the prostate. Magn Reson Imaging Clin N Am. 2008; 16(4):697–710. ix–x. [PubMed: 18926432]

125. Scheidler J, Hricak H, Vigneron DB, Yu KK, Sokolov DL, Huang LR, Zaloudek CJ, Nelson SJ, Carroll PR, Kurhanewicz J. Prostate cancer: localization with three-dimensional proton MR spectroscopic imaging--clinicopathologic study. Radiology. 1999; 213(2):473–480. [PubMed: 10551229]

126. Kurhanewicz J, Bok R, Nelson SJ, Vigneron DB. Current and potential applications of clinical 13C MR spectroscopy. J Nucl Med. 2008; 49(3):341–344. [PubMed: 18322118]

127. Aime S, Dastru W, Gobetto R, Santelia D, Viale A. Agents for polarization enhancement in MRI. Handb Exp Pharmacol. 2008; 185(Pt 1):247–272. [PubMed: 18626807]

128. Ardenkjaer-Larsen JH. Hyperpolarized 13C magnetic resonance imaging-principles and applicxations. Molecular Imaging: Principles and Practice. People's Medical Publishing House, Shelton CT. 2009:377–388.

129. Altes TA, Salerno M. Hyperpolarized gas MR imaging of the lung. J Thorac Imaging. 2004; 19(4):250–258. [PubMed: 15502612]

130. Oros AM, Shah NJ. Hyperpolarized xenon in NMR and MRI. Phys Med Biol. 2004; 49(20):R105–R153. [PubMed: 15566166]

131. Mansson S, Johansson E, Magnusson P, Chai CM, Hansson G, Petersson JS, Stahlberg F, Golman K. 13C imaging-a new diagnostic platform. Eur Radiol. 2006; 16(1):57–67. [PubMed: 16402256]

132. Golman K, Petersson JS. Metabolic imaging and other applications of hyperpolarized 13C1. Acad Radiol. 2006; 13(8):932–942. [PubMed: 16843845]

133. Viale A, Reineri F, Santelia D, Cerutti E, Ellena S, Gobetto R, Aime S. Hyperpolarized agents for advanced MRI investigations. Q J Nucl Med Mol Imaging. 2009; 53(6):604–617. [PubMed: 20016452]

134. Viale A, Aime S. Current concepts on hyperpolarized molecules in MRI. Curr Opin Chem Biol. 2010; 14(1):90–96. [PubMed: 19913452]

135. Albers MJ, Bok R, Chen AP, Cunningham CH, Zierhut ML, Zhang VY, Kohler SJ, Tropp J, Hurd RE, Yen YF, Nelson SJ, Vigneron DB, Kurhanewicz J. Hyperpolarized 13C lactate, pyruvate, and alanine: noninvasive biomarkers for prostate cancer detection and grading. Cancer Res. 2008; 68(20):8607–8615. [PubMed: 18922937]

136. Day SE, Kettunen MI, Gallagher FA, Hu DE, Lerche M, Wolber J, Golman K, Ardenkjaer-Larsen JH, Brindle KM. Detecting tumor response to treatment using hyperpolarized 13C magnetic resonance imaging and spectroscopy. Nat Med. 2007; 13(11):1382–1387. [PubMed: 17965722]

137. Ward CS, Venkatesh HS, Chaumeil MM, Brandes AH, Vancriekinge M, Dafni H, Sukumar S, Nelson SJ, Vigneron DB, Kurhanewicz J, James CD, Haas-Kogan DA, Ronen SM. Noninvasive detection of target modulation following phosphatidylinositol 3-kinase inhibition using hyperpolarized 13C magnetic resonance spectroscopy. Cancer Res. 2010; 70(4):1296–1305. [PubMed: 20145128]

138. Zierhut ML, Yen YF, Chen AP, Bok R, Albers MJ, Zhang V, Tropp J, Park I, Vigneron DB, Kurhanewicz J, Hurd RE, Nelson SJ. Kinetic modeling of hyperpolarized 13C1-pyruvate metabolism in normal rats and TRAMP mice. J Magn Reson. 2010; 202(1):85–92. [PubMed: 19884027]

139. Ellena S, Viale A, Gobetto R, Aime S. Para-hydrogen induced polarization of Si-29 NMR resonances as a potentially useful tool for analytical applications. Magn Reson Chem. 2012; 50(8):529–533. [PubMed: 22730263]

140. Merritt ME, Harrison C, Kovacs Z, Kshirsagar P, Malloy CR, Sherry AD. Hyperpolarized (89)Y offers the potential of direct imaging of metal ions in biological systems by magnetic resonance. J Am Chem Soc. 2007; 129(43):12942–12943. [PubMed: 17927188]

141. van Heeswijk RB, Uffmann K, Comment A, Kurdzesau F, Perazzolo C, Cudalbu C, Jannin S, Konter JA, Hautle P, van den Brandt B, Navon G, van der Klink JJ, Gruetter R. Hyperpolarized

lithium-6 as a sensor of nanomolar contrast agents. Magn Reson Med. 2009; 61(6):1489–1493. [PubMed: 19353663]

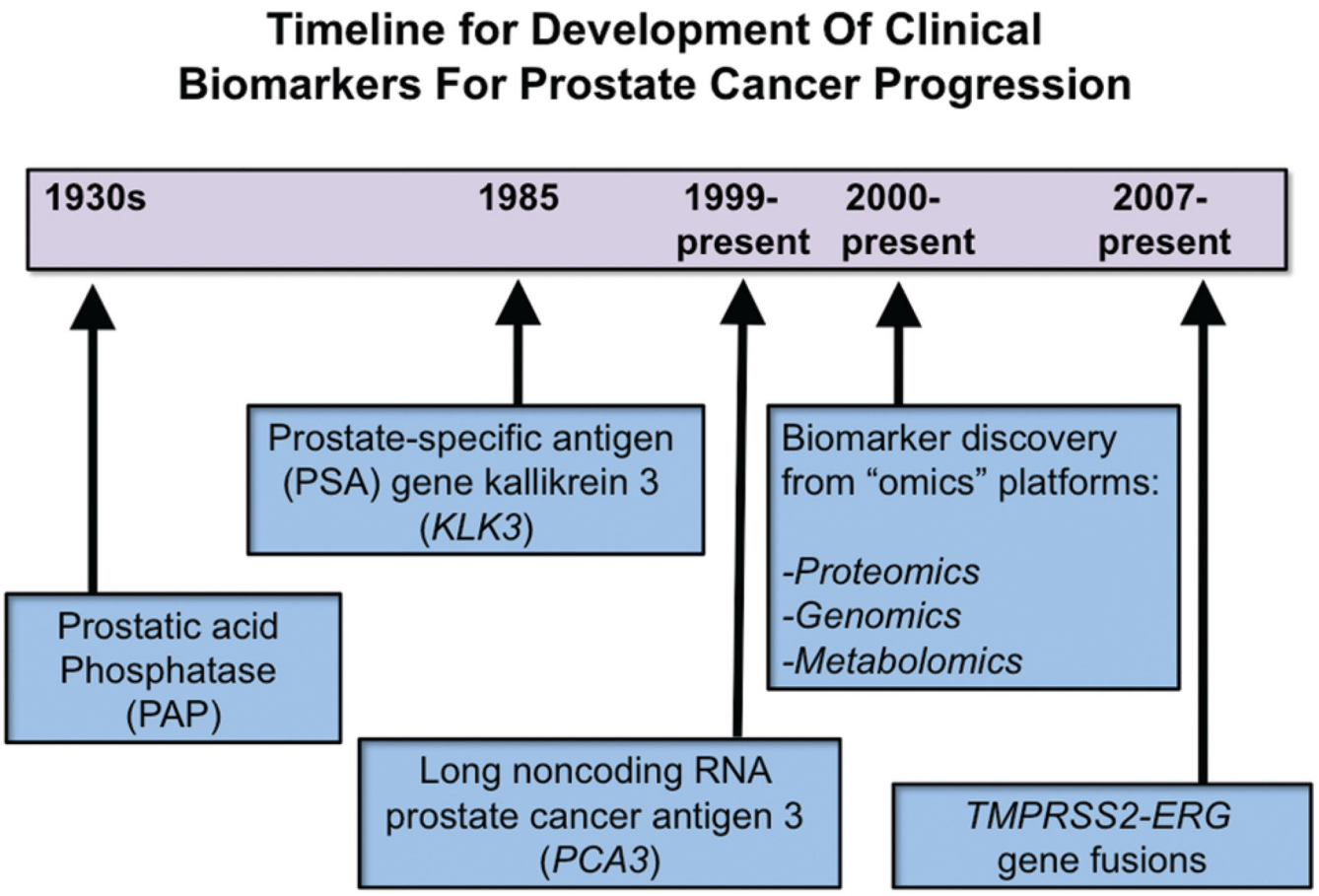

Figure 1.
Timeline for discovery of biomarkers used for detection and diagnosis of prostate cancer.

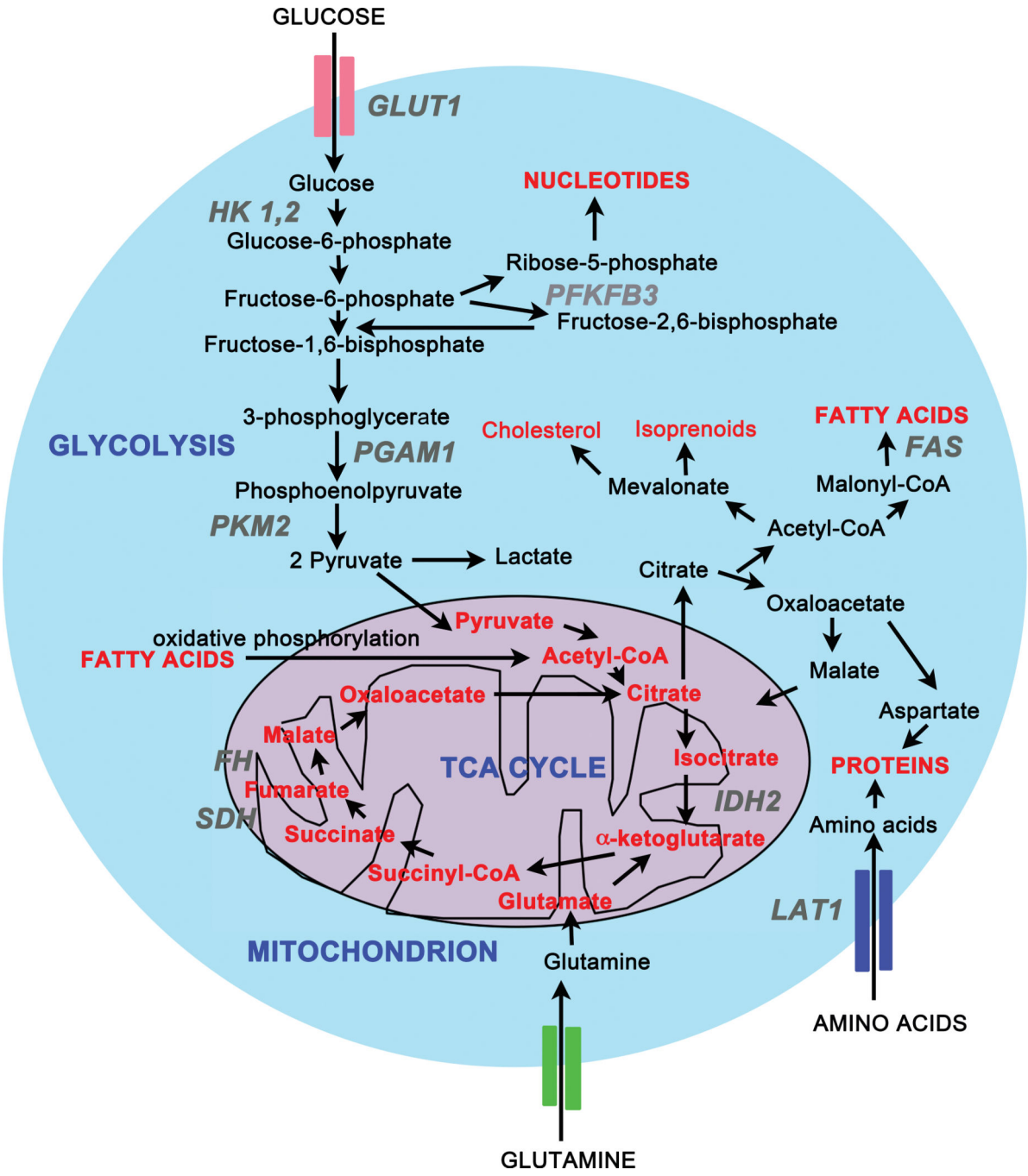

Figure 2. Cancer Metabolic Pathways involving Glycolysis and the TCA Cycle

Cells take up nutrients such as glucose, glutamine, and fatty acids to produce ATP. One mole of glucose is broken down into 2 moles of pyruvate, 2 moles of ATP, and 2 moles of NADH during glycolysis, which occurs in the cytoplasm. Pyruvate enters the mitochondrion where it is oxidized to Acetyl CoA, 2 ATP's, 8 NADH's, $2FADH_2$'s and $6CO_2$s per glucose molecule in the TCA cycle. Normal cells use the energy released from glycolysis and the TCA cycle for cellular processes. The TCA cycle also produces building blocks for synthesis of proteins, lipids, and nucleic acids, all of which are required for cell growth. In

contrast, cancer cells have increased uptake of glucose and glutamine to feed cell growth and proliferation. Enzymes and transporters that are either upregulated or mutated in cancer are shown in italics. These include the glucose transporter GLUT1, hexokinase 1,2 (HK 1,2), phosphoglycerate mutase 1 (PGAM1), pyruvate kinase M2 (PKM2), phosphofructo-2-kinase/fructose-2,6-bisphosphatase 3 (PFKFB3), isocitrate dehydrogenase 2 (IDH2), succinate dehydrogenase (SDH), and fumarate hydratase (FH). Adapted with permission from Lydia et al Cell Met. (2013), 17(3), p 466.

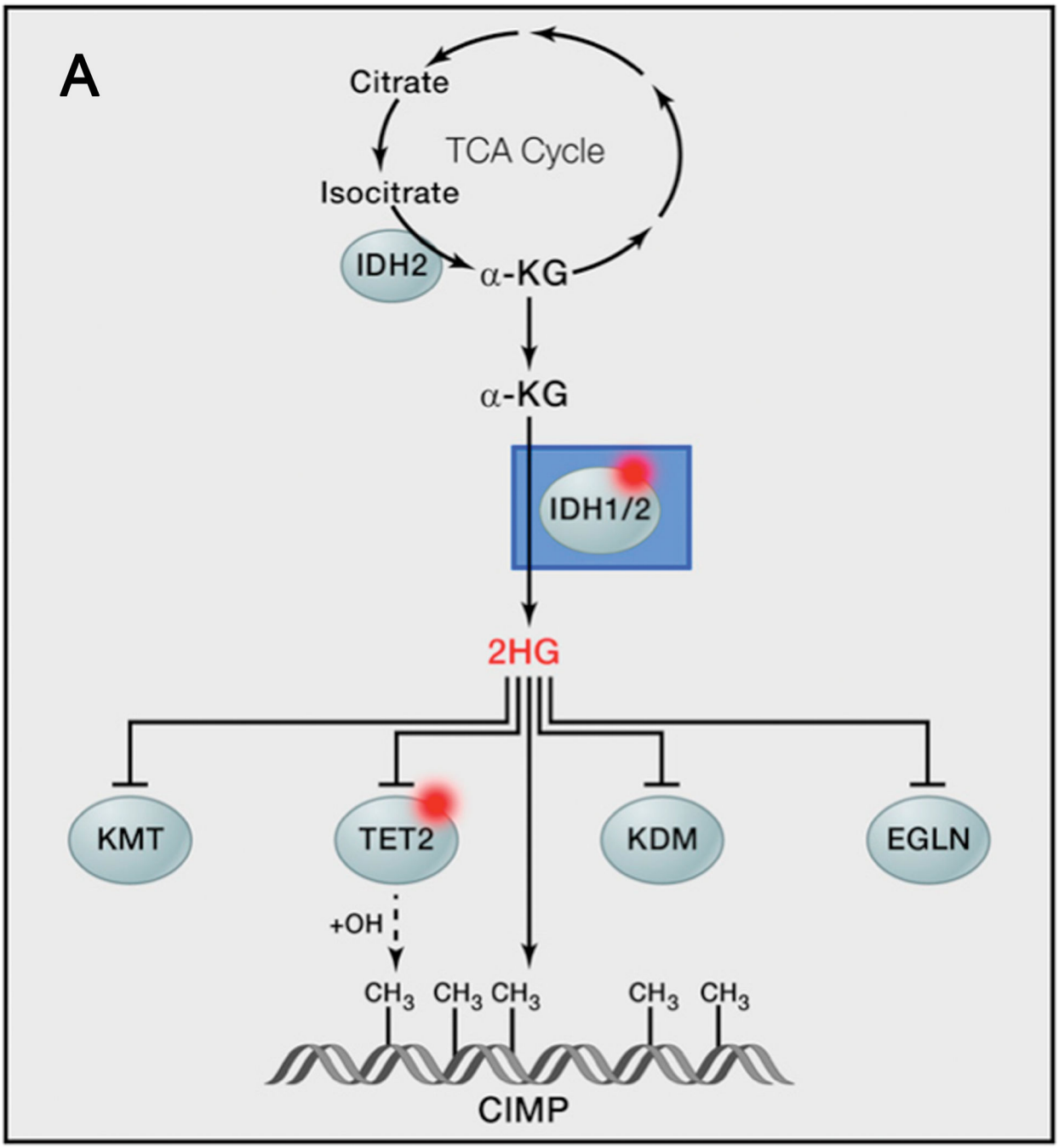

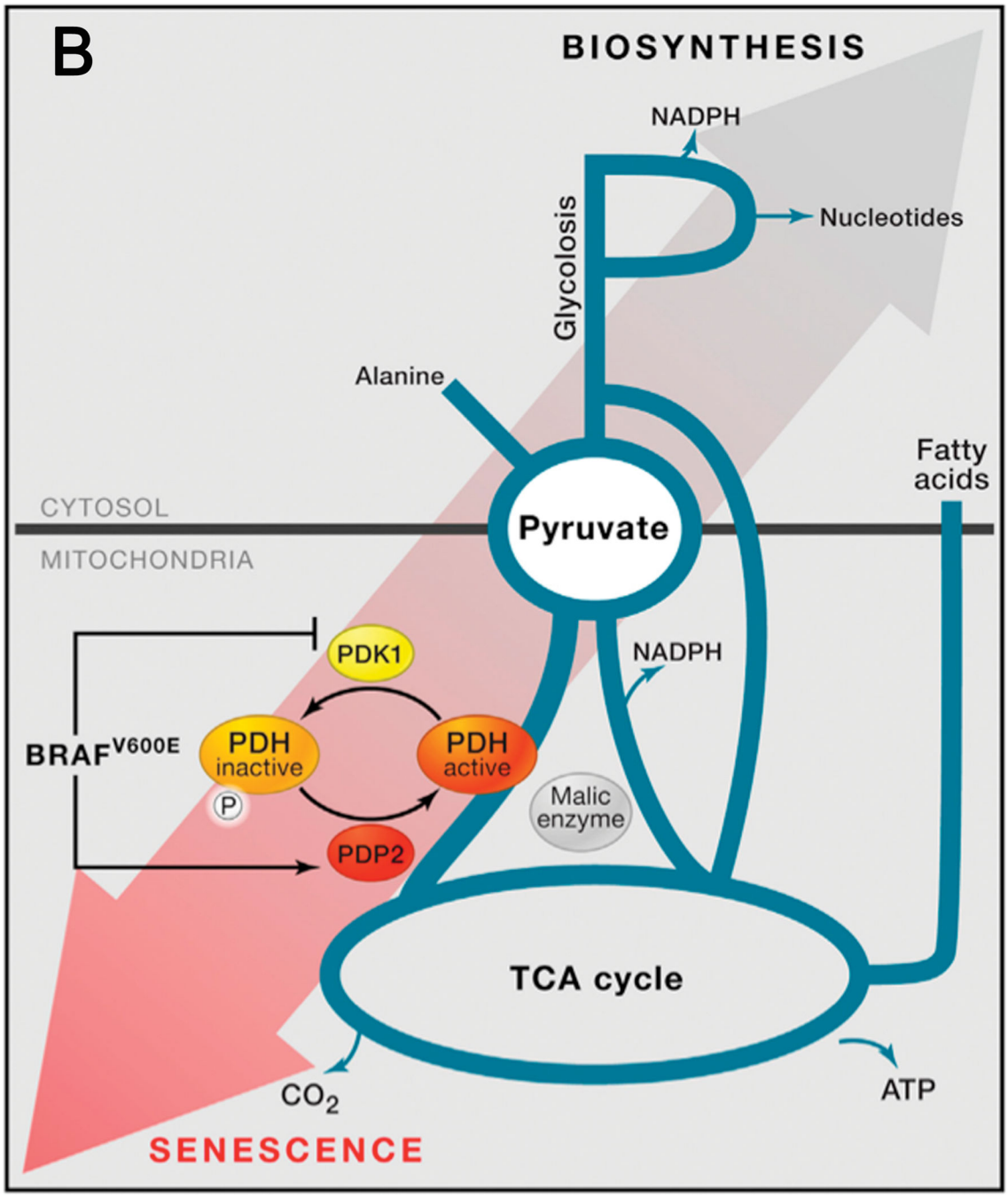

Figure 3.

(A) Somatic IDH1/2 mutations produce 2HG. The normal function of IDH1/2 is to oxidize isocitrate to α-ketoglutarate (α-KG), a component of the TCA cycle. However, mutant forms of IDH enzymes convert isocitrate to the R-enantiomer of 2-hydroxyglutarate (2HG). 2HG inhibits α-KG dependent enzymes downstream exerting effects on transcription and DNA methylation. Reproduced with permission from Garraway LA and Lander ES, Cell (2013), 153, pp. 17–37 Elsevier. (B) Pyruvate lies at a critical juncture, linking anabolic and catabolic pathways in metabolism. The enzymes PDH kinase 1 (PDK1) and PDH

phosphatase 2 (PDP2) regulate the pyruvate flux by controlling the activity of the pyruvate dehydrogenase complex (PDH). PDH controls the entry of pyruvate into the TCA cycle. High rates of pyruvate oxidation induce oncogene-induced senescence (OIS). Reproduced with permission from Olenchock BA and Vander Heiden MG, Cell (2013), 153, pp. 1429–1430 Elsevier.

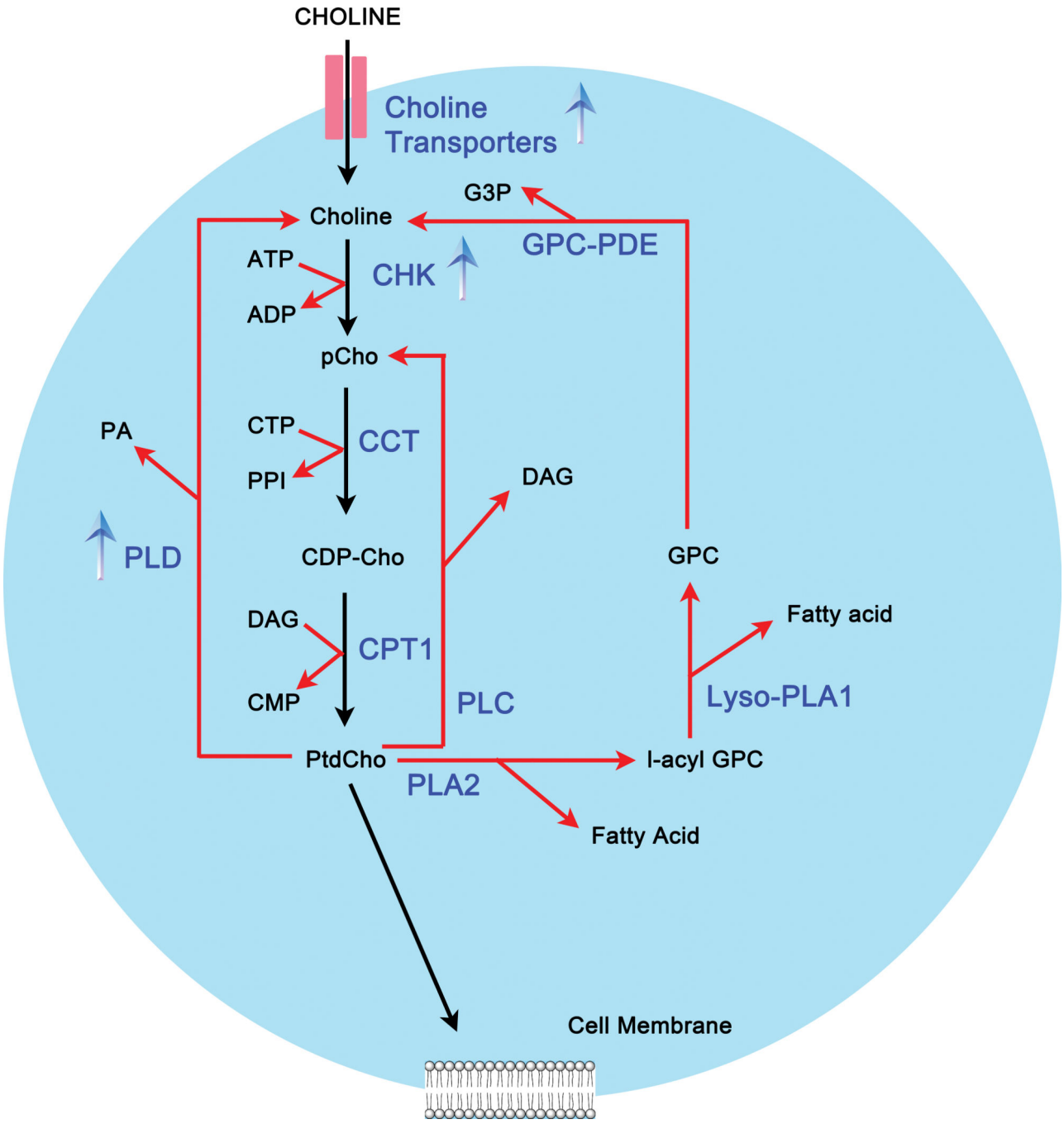

Figure 4. Choline phospholipid metabolism in the cell

Choline is taken into the cell by choline transporters that are upregulated in cancer. The biosynthesis of choline cycle metabolites by the Kennedy pathway (also called the CDP-choline pathway) is shown in black arrows. The catabolism of choline metabolites is shown in gray arrows. The metabolites are phosphocholine (pCho), cytidine diphosphate choline (CDP-Cho), and phosphatidylcholine (PtdCho). Choline kinase (CHK), the enzyme that catalyzes the phosphorylation of choline to pCho is also upregulated in cancer. The reaction catalyzed by CTP-phosphocholine cytidylyltransferase (CCT) is the rate-limiting step.

Finally, conversion of CDP-Cho to PtdCho is mediated by 1,2-diacylglycerol cholinephosphotransferase (CPT1). PtdCho is degraded to choline by phospholipase D (PLD), an enzyme that is also upregulated in cancer cells. Other enzymes that are involved in the conversion of PtdCho to choline are phospholipase A2 (PLA2) that yields 1-acylglycerophosphocholine (1-acyl GPC), lyso-phospholipase A1 (lyso-PLA1) that converts 1-acyl GPC to GPC, and finally the enzyme GPC phosphodiesterase (GPC-PDE) converts GPC to choline.

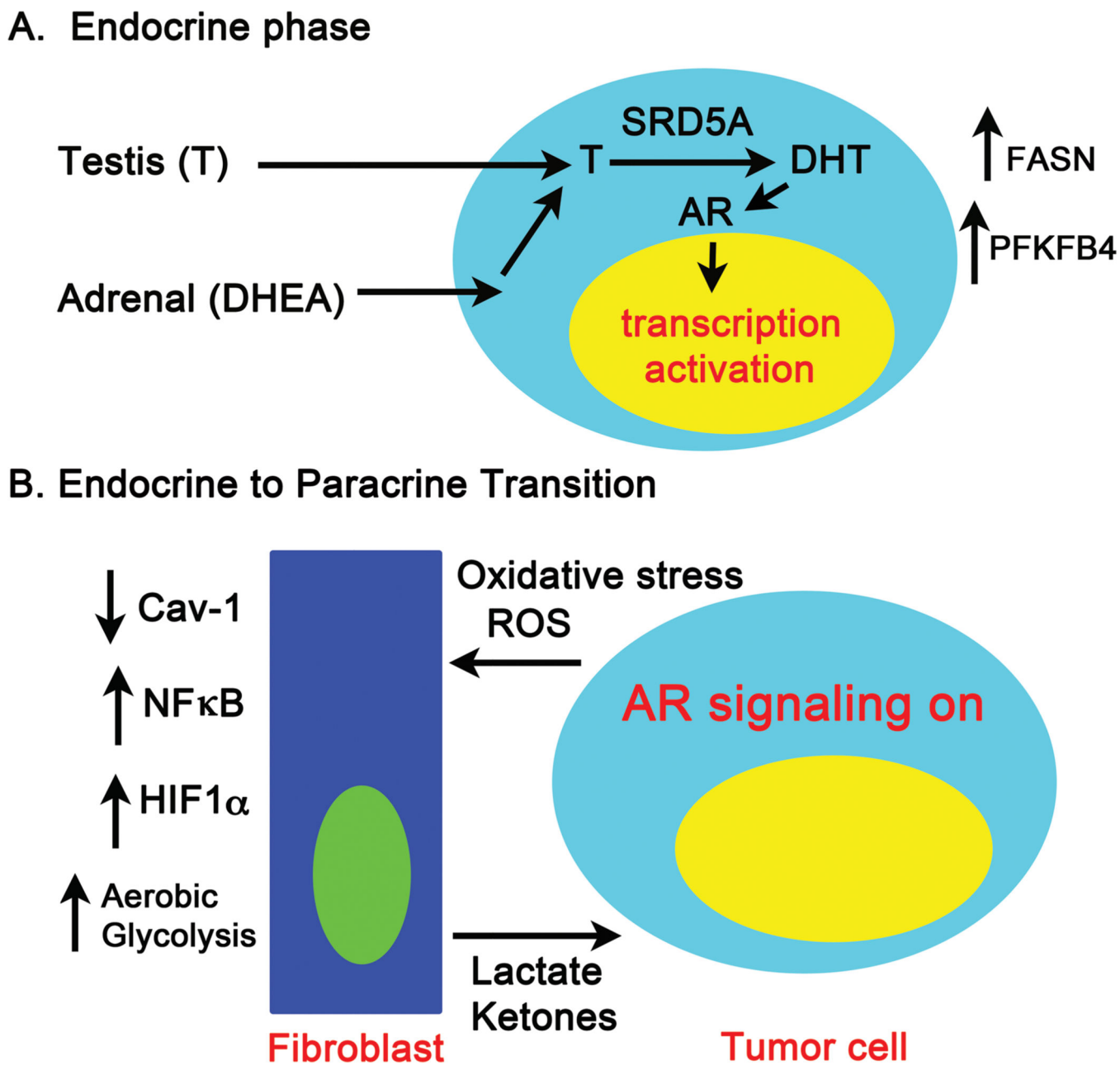

Figure 5.

Histopathologic stage pT3a prostate cancer, Gleason score 5, in a 58-year old man. (A) Fast spin-echo T2-weighted (5000/102) transverse MR image through the middle gland was obtained with an endorectal coil. A tumor focus (arrows) is seen as an area of decreased signal intensity in the peripheral zone of the right gland. (b) The same section as in (A) shows areas of definite cancer, as demonstrated with 3D MRSI findings overlaid and circled. Note the concordance between (A) and (B). (C) MR spectrum obtained from area of imaging abnormality in the right peripheral zone demonstrates elevated choline and reduced citrate, a pattern consistent with definite cancer. (D) MR spectrum obtained from a normal left peripheral zone demonstrates a normal spectral pattern with citrate dominant and no

abnormal elevation in choline. Reproduced with permission from Scheidler et al. Radiology (1999), 213 (2), pp. 473–480 RSNA.

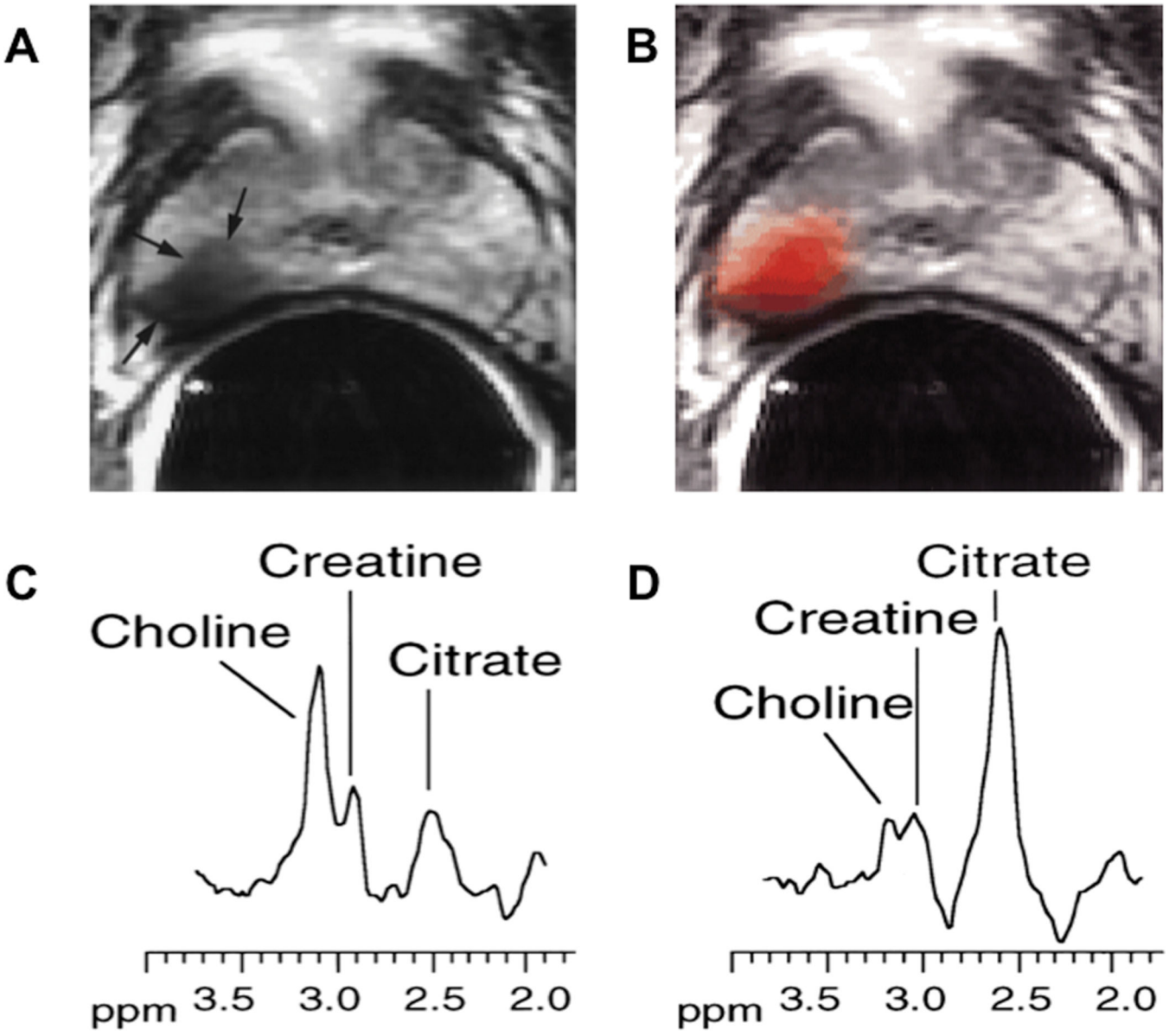

Figure 6.